IST-2000-30148 I-METRA

D6.1

Implications in Re-configurable Systems beyond 3G

(Part 1)

Contractual Date of Delivery to the CEC: 31 August, 2003

Actual Date of Delivery to the CEC: 31 October, 2003

Author(s): Lars T. Berger, Javier R. Fonollosa, Luis García, Alba Pagès-Zamora, Juan Ramiro-Moreno

Participant(s): AAU, UPC

Work package: WP6: Implications in Re-configurable Systems beyond 3G

Est. person months: 6

Security: Public

Nature: Report

Version: 1.0

Total number of pages: 54

Abstract:

In this activity MIMO HSDPA is evaluated as the UMTS evolution that could allow a combination of high bit rate services, coverage and mobility with a good trade-off between cost and performance. This evaluation requires the definition of an objective framework for comparison between competing air interface technologies for Systems beyond 3G, and should be carried out in cooperation with other IST projects.

The deliverable is complemented by analytically assessing channel capacity in flat Rician- and Rayleigh fading when ideal proportional fast scheduling, optimal rate adaptation, and various transmit diversity techniques are used.

Keyword list: UMTS, MIMO, HSDPA, ODMA, HIPERLAN/2,

EXECUTIVE SUMMARY

In this activity MIMO HSDPA is evaluated as the UMTS evolution that could allow a combination of high bit rate services, coverage and mobility with a good trade-off between cost and performance. This evaluation requires the definition of an objective framework for comparison between competing air interface technologies for Systems beyond 3G, and should be carried out in cooperation with other IST projects.

The deliverable is complemented by analytically assessing channel capacity in flat Rician- and Rayleigh fading when ideal proportional fast scheduling, optimal rate adaptation, and various transmit diversity techniques are used.

DISCLAIMER

The work associated with this report has been carried out in accordance with the highest technical standards and the I-METRA partners have endeavoured to achieve the degree of accuracy and reliability appropriate to the work in question. However since the partners have no control over the use to which the information contained within the report is to be put by any other party, any other such party shall be deemed to have satisfied itself as to the suitability and reliability of the information in relation to any particular use, purpose or application.

Under no circumstances will any of the partners, their servants, employees or agents accept any liability whatsoever arising out of any error or inaccuracy contained in this report (or any further consolidation, summary, publication or dissemination of the information contained within this report) and/or the connected work and disclaim all liability for any loss, damage, expenses, claims or infringement of third party rights.

1 INTRODUCTION: CURRENT ACTIVITIES IN SB3G

In this section we summarise the vision of Systems Beyond 3G of some of the organisations and forums with recognised activity in the area, paying special attention to the impact on the physical layer.

1.1 SB3G Vision in WWRF

WWRF vision of SB3G is dominated by their well-known Multi Sphere Level Concept with little implication on the specific air interfaces of the underlying technologies. Emphasis is given to the connectivity and to the satisfaction of user's needs. A brainstorming exercise was undertaken [COST 273] to define what wireless challenges are presented by the different spheres in the model.

	Issue				
Sphere	Wireless?	Capacity	Interference	Coverage	Battery Pwr.
PAN	✓[1]	×	×	×	**?**
Immediate Environment	✓	✓	✓	✓	×
Instant Partners	✓	✓	✓	×	×
Radio Access	✓	✓	✓	✓	✓
Interconnectivity	**?**[2]	✓[2]	×	×	×
Cyberworld	×	**N/A**	**N/A**	**N/A**	**N/A**

Table 1. Limitation identification in multisphere concept [COST 273].

Notes 1: A PAN could be used to form a virtual antenna array
2: In general interconnectivity is considered to be a higher layer issue. However the backhaul for some systems may be provided by a wireless link (e.g. HAPs, microwave links in GSM/UMTS networks).

Different radio technologies are likely to enable the various concepts and so each different scenario could lead to a unique MIMO solution, if such an enhancement is required. This would present challenging implementation problems. In any case WWRF supports the Systems beyond IMT-2000 vision of ITU illustrated in the classic Mobility versus Data Speed diagram (Figure 1).

1.1.1 Data Rates Estimates and Range Calculations for new Elements of Systems Beyond IMT-2000

During the sixth WWRF meeting a Research Item was presented entitled "Data Rates Estimates and Range Calculations for new Elements of Systems Beyond IMT-2000" [WWRF 6 Mohr]. As a target figure, it was suggested that Systems beyond IMT-2000 should be able to cope with average data rates in the order of 0.1 to 1 Mbps per user session and offer peak rates in the order of 10 to 20 Mbps. The aggregate cell capacity is envisioned (in a compromise between economics and performance) in the order of 25 to 50 Mbps. Estimated figures of average traffic demand per user and subscriber density are employed to derive an estimated traffic demand per area of 1 to 200 Mbps/km^2. These requirements are illustrated in Table 2.

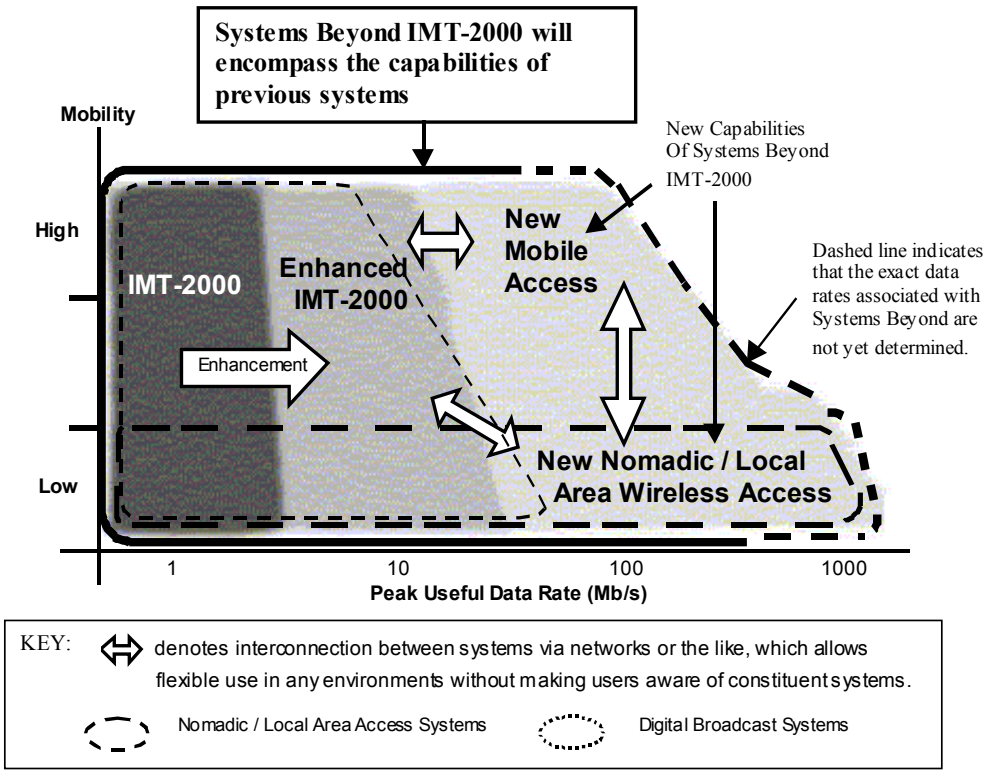

Dark gray color indicates existing capabilities, medium gray color indicates enhancements to IMT-2000, and the lighter gray color indicates new capabilities of Systems Beyond IMT-2000.

The degree of mobility as used in this figure is described as follows: Low mobility covers pedestrian speed, and high mobility covers high speed on highways or fast trains (60 km/h to ~250 km/h, or more).

Figure 1. Illustration of Capabilities of IMT-2000 and Systems Beyond[1]

Parameter	Estimated minimum	Estimated maximum
Peak user data rate (Mbps)	10	20
Average user data rate (Mbps)	0.1	1
Aggregate cell capacity (payload Mbps)	25	50
Traffic demand per area (Mbps/km^2)	1	200

Table 2. Estimated requirements for Systems Beyond IMT-2000 [WWRF 6 Mohr].

These basic requirements are analysed, assuming a single carrier[2] system employing 100 MHz available bandwidth, for different combination of modulation and coding schemes and for different propagation models in order to provide realistic estimated cell sizes. It is concluded that sufficient coverage can not be guaranteed in all environments using reasonable cell sizes. For example, an aggregate cell capacity (payload) of 100 Mbps can be obtained using QPSK and coding rate c_r= ½. However, the outdoor maximum cell size can range between 1870 m

[1] Source: ITU-R WP8F, 7th Meeting Ottawa, 29 May - 5 June 2002, TEMP 316-E.
[2] Similar results are expected for a multicarrier system employing the same bandwidth.

and 123 m and between 659 m and 50 m depending on the propagation model and assuming no wall penetration or single wall penetration respectively (see Table 7 in [WWRF 6 Mohr]). This short coverage implies also a minimum cell capacity per area much higher than required (e.g 1.3 Gbps/ km^2 for a cell with 3 sectors and 300m cell range)

According to the authors of the document, these figures indicate that deployment of systems beyond IMT-2000 requires new strategies and system architectures in order to provide quasi line-of-site propagation using multihop or repeater concepts as illustrated in Figure 2 so that deployment cost can be reduced significantly.

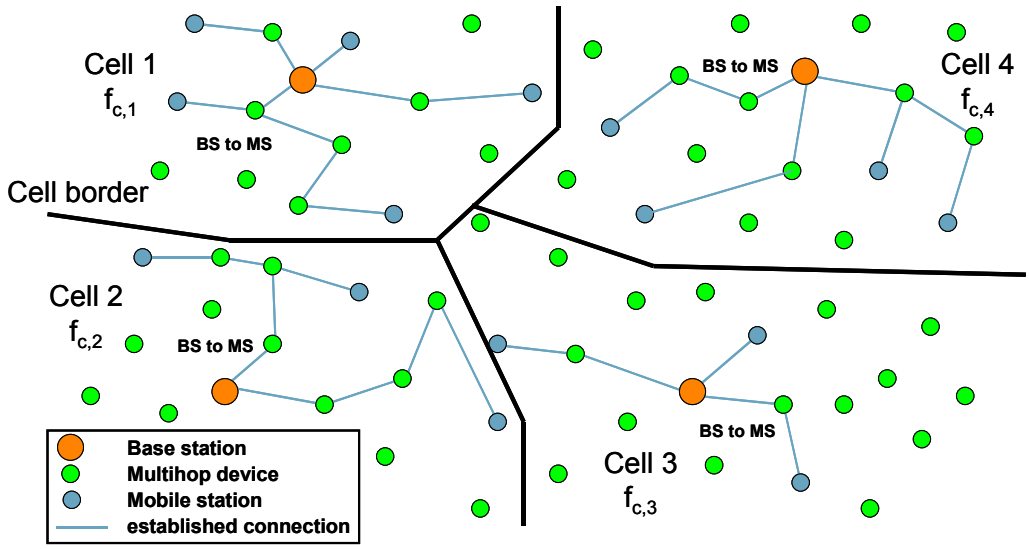

Figure 2. Basic system architecture for Systems Beyond IMT-2000 [WWRF 6 Mohr]

The application of MIMO solutions within a multi-hop system could provide enhancement through:

- Increased capacity at the data sink. Relay systems will tend to concentrate capacity requirements on the last hop – between MS and BTS – and MIMO may prevent this from becoming a significant performance bottleneck
- Increased data rate over the links
- Increased range of the links thereby reducing the number of required hops and decreasing the complexity of the routing algorithms

1.1.2 Adaptive Antenna work item in WWRF

The New Technologies Working Group of WWRF includes the Adaptive Antenna work item for which a white paper has been drafted [WWRF_WG4_SA]. Smart Antennas are presented as a technology able to *achieve significantly higher data rates, better link quality, and increased spectral efficiency*. This document provides an introduction to Smart Antenna and MIMO processing and focuses on well-known issues like realistic performance evaluation, reconfigurability, robustness and implementation complexity. There is no indication, however, on explicit requirements that would allow this technology, when implemented on specific air interfaces, to become a key enabler of Systems beyond 3G.

1.2 SB3G Vision in the SB3G Cluster of IST Projects.

This cluster released in March 2002 the report "A vision of Systems Beyond 3G", Release 2001 [SB3G Vision] which combined the vision of each of the projects participating in the cluster. The report includes a project description and an overview of the key technologies of the contributing projects. Only two pages (out of 83) are devoted to Physical Aspects of key technologies including contributions from the projects DRIVE, ADAMAS, EMBRACE, WIND-FLEX and BRAIN. Again, detailed physical layer requirements for the emerging technologies in SB3G are missing and are vaguely justified by the *demand for cost-effective delivery of broadband services over resilient broadband networks.*

More specifically, the DRIVE project, which addresses the convergence of cellular and broadcast networks, emphasises the following areas:

- Dynamic spectrum allocation (DSA)
- Cooperation of different radio access systems (GSM, GPRS, UMTS, WLAN, DAV, DVB)
- Asymmetric usage of spectrum
- Adaptive, scalable and modular applications

The ADAMAS project proposes a new OFDM based air interface for outdoor broadband fixed wireless systems which employs adaptive modulation and dynamic allocation schemes.

BRAIN has adapted HIPERLAN/2 in order to provide full QoS support for real and non-real time services in hot-spot areas enhancing its MAC and network layer functionalities.

One can then conclude that the vision of the SB3G Cluster is mostly related to improvement of current systems so that they become more efficient and allow for seamless connectivity including enhancements or new definitions of physical layer specifications.

1.3 SB3G Vision of the IST Project MIND.

MIND was focused on developing a new air interface to meet the requirements of potential 4G systems. As such MIND concentrated on definition of technologies that are necessary for operating wireless networks in an ad-hoc, self-configured and adaptive fashion. Three basic scenarios are defined [MIND D3.2]:

- Mobile ad-hoc extensions with multi-hop support: Centralised and (partially) distributed controlling.

- Outdoor rooftop wireless routers

- Multi-hop Vehicle to Vehicle communication

The project then concentrates in developing both the physical layer and the MAC layer techniques. They would allow HIPERLAN/2 to operate under these scenarios. They also

include support for dynamic topologies, much wider coverage and much higher mobility than the traditional wireless LAN environment.

MIND seek to demonstrate how an enhanced HIPERLAN/2 system is able to fill the gap between the high mobility and moderate bit rate of UMTS and the low mobility and high bit rate of current WLAN systems.

1.4 "Analysis of OFDM for UTRAN enhancement" Study Item in 3GPP

A Study Item was launched in 3GPP TSG RAN related to the evaluation of possible use of OFDM in UTRAN [R1-02-1195]. The motivation was based on the availability of the technology, already developed for other systems (i.e. DAB, DVB-T, 802.11a) in order to provide enhanced performance for high bit rate services. However, it should be noted that OFDM is to be considered as one option for the enhancement of UTRAN, not as a sole candidate. Specifically, the Study Item is specified as:

The objective of this Study Item is to study the applicability of OFDM in UTRAN and its potential to enhance UTRAN.

It should be possible to use OFDM in a 5MHz spectrum allocation. As a starting point, OFDM will be considered in the downlink only.

The use of OFDM should have the minimum impact on current protocols. Changes other than those needed to introduce the signalling necessary to support a new modulation in UTRAN will not be considered.

The following list provides examples of areas that may be considered in the study:

- *Throughput for data services. To be compared with throughput of current UTRAN releases*
- *Various options of UE receiving OFDM carrier in combination with Release 99/Release 5 UMTS*
- *Support for MIMO and other advanced antenna array techniques*
- *Support for personal, multimedia and broadcast services*
- *Deployment scenarios, including frequency reuse aspects, within diverse spectrum allocations*

The study should consider performance aspects, aspects linked to the evolution of UMTS (high level architecture, diverse spectrum arrangements and allocations), impact on signalling in UTRAN, aspects of capacity/cost/complexity/coverage and aspects of co-existence with the existing UTRAN releases.

The output of the study item will be a Technical Report containing an analysis of the feasibility and potential benefits of introducing OFDM in UTRAN, and a recommendation to RAN Plenary on a potential work item time-frame and work plan.

Although the final scope of the study is still undefined, there are some similarities between the intention of this study item and the work currently carried out in MIND (see Section 1.3). The objective is to evaluate how an OFDM based air interface can provide high bit rates and mobility and therefore outperform current HSDPA UTRA specifications.

1.5 Summary of current situation

In the previous sections a number of visions for SB3G were outlined. These could be broadly grouped into three views:

1) **Convergence** – this arose from the future perceived users requirement for "any time, any where, any how" access to communication, services and content. From a technology perspective this requires seamless interaction of different technologies and will probably imply increased resources.

2) **3G evolution** – enhancements to current 3G technologies will supply sufficient capacity and data rates to meet future demands.

3) **4G Cellular** – a new air interface may be required to meet future traffic demands. Key technologies may include multi-hop relaying, multi-carrier modulation and antenna array processing (MIMO or smart antennas).

2 TASK 1A. DEFINITION OF A FRAMEWORK FOR COMPARISON BETWEEN POTENTIAL AIR-INTERFACE PROPOSALS.

This task aims at developing a common set of specification for harmonisation of link level results among different IST projects. As such it shares one of the main objectives of the Broadband Air Interfaces Cluster initiated in December 2002. The main justification comes from the need for higher data rates in future wireless communications in which it is likely that different air interfaces will co-exist for the different needs in terms of mobility, range, etc. Activities in this cluster could provide a significant contribution towards clarifying the merits and weaknesses of different air interfaces identifying preferential applications for the different access mechanisms.

During the second BAI cluster meeting that took place on March 12th 2003 the following table of basic link simulation parameters was agreed between the projects dealing with UMTS evolution scenarios.

Common Scenario	I-METRA	MATRICE	FITNESS	ROMANTIK
Targeted standard	UMTS++	4G Cellular	UMTS++	UMTS++
Objectives	Throughput vs Range	Throughput	Reconfigurability	Throughput & Reconfigurability
Frequency	2 & 5 GHz	5 GHz	2 & 5 GHz	2 & 5 GHz
Bandwidth	5 & 20 MHz	50 MHz	5 MHz	5 & 20 MHz
Type of service	Packet	Packet	Packet	Packet
Max User Bit Rate	40 Mbps	50 Mbps	20 Mbps	40 Mbps
Max No of antennas	4x4	tbd	4x4	4x4
Mobility (Indoor/Outdoor) (Min-Max km/h)	3(O)-120(O)-300(O)	3(I)-300(O)	3(O)-120(O)	3(I&O)-50 (O)
UL/DL	UL/DL	UL/DL	DL	UL/DL
Duplex	FDD	TDD	FDD	FDD & TDD
Channel models	I-METRA	3GPP2/LT	3GPP1/3 (Geometry based stochastic)	TBC
HW platform	NO	YES (BB, TI DSP, XILINX FPGAs)	YES (RF & BB)	NO

Table 3. Parameters agreed for simulation harmonisation.

Table 3 represents the first step towards objective simulation comparison and has derived in a bilateral collaboration with the project FITNESS described in the following section.

2.1 Extension of HSDPA to 20 MHz bandwidth. A harmonised scenario with the project FITNESS.

One of the main objectives of the BAI cluster is to promote the harmonisation of link simulation parameters in order to allow meaningful comparison between project results. In this context, and considering the common 20MHz bandwidth of the I-METRA MIMO HSDPA extension and the MIMO HYPERLAN/2 simulations of FITNESS, an activity was initiated in order to harmonise, as much as possible in different systems as UTRA HSDPA

and HYPERLAN/2, other basic simulation parameters. The outcome of this process is described in the following table.

Project	**FITNESS**	**I-METRA (20 MHz)**
MIMO Configuration	2x2, 4x4, other	2x1, 2x2
Gross bit rates	6,12,24,36,54 Mbps	9.6, 19.6 Mbps
Coding type	½ and ¾ Convolutional	½ Turbo
Modulation	BPSK, QPSK	QPSK, 16QAM
Packet length	864	5114 bits
Packet duration	≤ 72 μs	~ 2ms/4 = 500 μs
Channel model	Close to ETSI BRAN C and E at 1.8 and 3 Km/h	ETSI BRAN A, C, D and E at 3 Km/h

Table 4. Basic link simulation parameters of FITNESS HYPERLAN/2 and I-METRA HSDPA 20 MHz extension.

It is apparent in this table that, although some level of harmonisation is possible with respect to MIMO antenna configuration and gross bit rates, there are some significant discrepancies with respect to aspects linked to the HYPERLAN/2 and HSDPA system parameters, like packet length and duration. Still, the link and throughput results provided in Deliverable D6.2 Implications in Re-configurable Systems beyond 3G (Part 2) represent a meaningful basis for comparison between simulations of both projects.

The I-METRA link-level MIMO channel simulator has also been upgraded to support the investigation of the extension of HSDPA to higher bandwidths. The time dispersion has been modeled according to the HiperLAN parameters published by Medbo et al [22]. The spatial parameters (AS, AoA/AoD) have been derived from the original 3GPP cases by triplicating the values of these 6-tap cases to the new 18-tap cases. Other choices of spatial parameters can easily be implemented by a simple modification of the parameter file describing the scenarios.

3 TASK 1B. INTERACTION OF FAST PACKET SCHEDULING AND TX-/RX-DIVERSITY

In Task 1b.) the network performance of a WCDMA system implementing the High Speed Downlink Packet Access (HSDPA) [3] concept of UMTS, which is introduced as a part of Release 5, is evaluated when different transmit and receive diversity techniques are deployed. Such evaluation is conducted primarily by means of dynamic network simulations; although a simplified theoretical analysis is also shown in order to further motivate the observed phenomena.

As part of the HSDPA concept, the introduction of many different advanced antenna techniques is being discussed within the 3GPP standardisation framework. In general, these techniques can be classified into two main groups. The first one focuses on adding diversity protection (by suppressing deep fades) and, in some cases, increasing the average energy-per-symbol-to-noise ratio (E_S/N_0) experienced by a single-stream link between the Node-B and the UE. The second one implements the so-called information multiple-input-multiple-output concept [5]. Such a concept requires the deployment of several antennas at both the Node-B and the UE, and relies on the spatial decorrelation of the radio channel matrix in order to achieve several parallel data streams within the same channelisation code. This study is concentrated on the first of the two aforementioned groups. Furthermore, within all the possibilities that fit into this group, the scope is further narrowed down, so that only those advanced antenna techniques that are already part of the Release 99 specifications are analysed. Although these techniques are already part of the Release 99 specifications, the analysis of their performance within the HSDPA framework is of paramount importance. The reason is that the mechanisms that lead to an eventual capacity increase are different from the case of Release 99, and so are the limitations that the system-specific aspects impose when taking profit out of the achieved E_S/N_0 improvement. For example, in Release 99, the deployment of dual antenna Rake receivers can easily lead to a situation in which the system becomes hard blocked due to lack of sufficient channelisation code resources [6] [21]. In HSDPA, this deployment triggers a more frequent use of higher modulation orders, which increase the bit rate at the expense of lower spectral efficiency. However, in HSDPA the aforementioned limitations are translated into some performance penalties, rather than hard blocking the system. This is the reason why such phenomenon is often referred to as soft code limitation.

For this study, three transmission schemes are considered at the Node-B: (i) single antenna transmission, (ii) two branch open loop space time transmit diversity (STTD) [4], and (iii) two branch closed loop transmit diversity (CLTD) mode-1, as described in [2]. At the UE, both single and dual antenna Rake receivers (2Rake) using maximal ratio combining (MRC) [1] are studied. Finally, the combination of transmit diversity at the Node-B and 2Rake at the UE is investigated.

As shown along this subsection, the performance of each advanced transmit and receive diversity technique is extremely dependent on the adopted packet scheduling strategy. This dependence is analysed in this study, and the obtained conclusions are compared to the ones obtained in some other studies, e.g., the ones presented in [7] [20]. Moreover, a simple

theoretical analysis is shown in order to provide an intuitive explanation for the trends that are observed in the system performance.

Task 1b.) is organised as follows. Subsection 3.1 shows a simple theoretical discussion about the interactions between multi-user diversity and other kinds of diversity, together with the expected impact of the UE speed on the performance of schedulers based on instantaneous knowledge of the radio channel. The system model and simulation assumptions are described in Subsection 3.2. In Subsection 3.3, the simulation results are shown and discussed. Finally, concluding remarks are given in Subsection 3.4.

3.1 Multi-user diversity, antenna diversity and UE speed

This subsection shows a simple theoretical discussion about the interactions between multi-user diversity and other kinds of diversity, together with the expected impact of the UE speed on the performance of schedulers based on instantaneous knowledge of the radio channel.

Let us assume a set of UEs with an infinite amount of data to transmit, which have to be served through a single time-shared channel. In order to exploit the multi-user diversity, the system serves the UE with the maximum normalised instantaneous channel quality. In other words, the system aims at scheduling the UEs when they are experiencing constructive fading. For this simple discussion, the instantaneous channel quality is defined by the instantaneous value of the corresponding fast fading process.

Moreover, for a certain time instant, the effective fading at the shared channel is defined as the instantaneous fading affecting the served UE. Under ideal instantaneous selection of the served UE, the effective fading process is the one resulting from selection combining of the fading processes of all the UEs in the cell [1].

The CDF of the effective fading process experienced at the shared channel in a single path propagation environment is depicted in Figure 3.1. Note that, for this theoretical discussion, each path is assumed to be Rayleigh distributed. In this plot, it can be seen that a larger number of UEs involves larger diversity protection, which is translated into a steeper CDF of the experienced fading on the shared channel.

This Figure also depicts information for the case in which STTD is enabled as a transmission technique. Note that STTD has been modelled by assuming that the fading process of one UE equals the average of two independent single antenna fading processes. As it can be seen, the deployment of STTD makes the CDFs steeper, which means that the diversity protection is increased even for a single UE. As a consequence, the achieved improvement from having multi-user diversity is smaller. In general, the higher the diversity order, the lower benefit can be obtained from extra sources of diversity [1].

The diversity protection provided by STTD is noticeable in two ways. On one hand, the probability of experiencing a deep fade is lowered. On the other hand, the strength of the constructive fades is statistically lower.

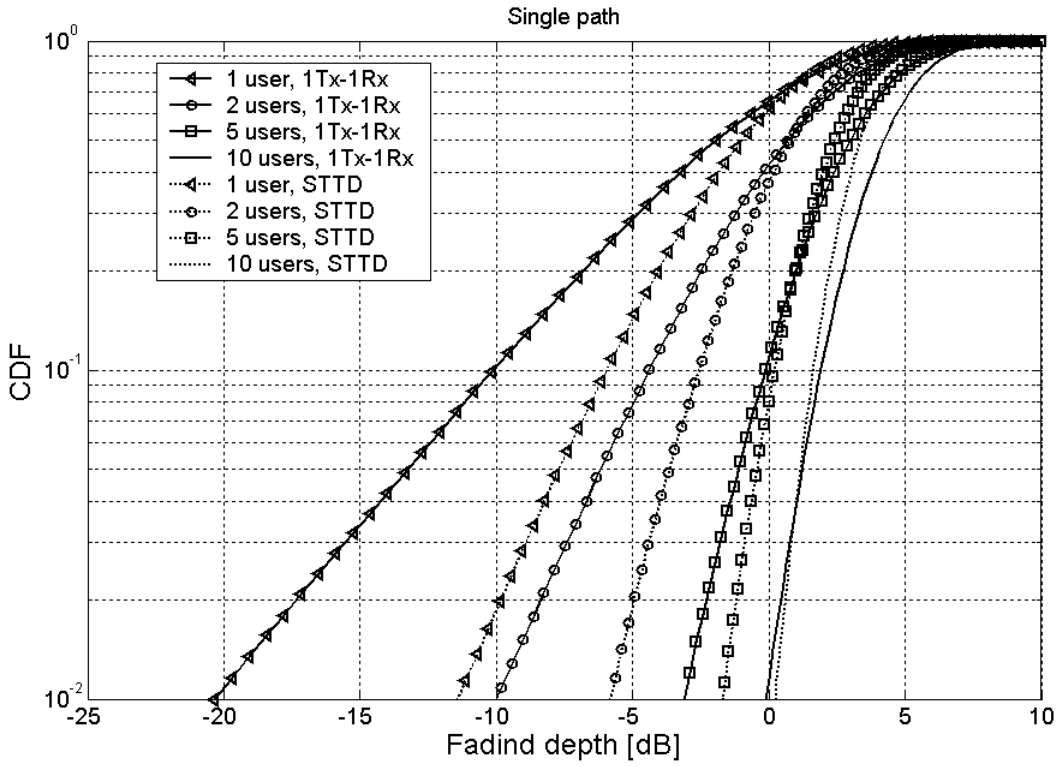

Figure 3.1 CDF of the effective fading process experienced at the shared channel for a single path propagation environment.

In a scenario in which the system tries to schedule UEs when they are experiencing constructive fading, the deployment of mechanisms (such as STTD) that stabilize the radio channel may not be beneficial, especially when the system has a sufficiently large amount of UEs among which to choose. In this case, it is very likely that most times there is at least one UE with a good instantaneous channel quality. As stated before, the instantaneous channel quality of a UE on the top of a fade is statistically worse when STTD is enabled. Thus, the answer on whether it is beneficial or not to deploy STTD depends on the number of UEs available for the selection combining process. For example, when there are few UEs among which to choose, it is not unlikely that the "best" UE is still experiencing destructive fading, which would allow STTD provide some performance improvement by fade suppression. All these mechanisms are illustrated in Figure 3.2, where the effective fading depth experienced in the shared channel is shown for different outage levels as a function of the number of UEs involved in the selection process.

As can be seen, as the number of UEs grows, the effective fading statistics of the shared channel improve more for the single antenna case than for STTD, which suggests that, from a certain number of UEs onwards, the system performance is better for the single antenna case. This conclusion is in coherency with the results shown in [7] and [20].

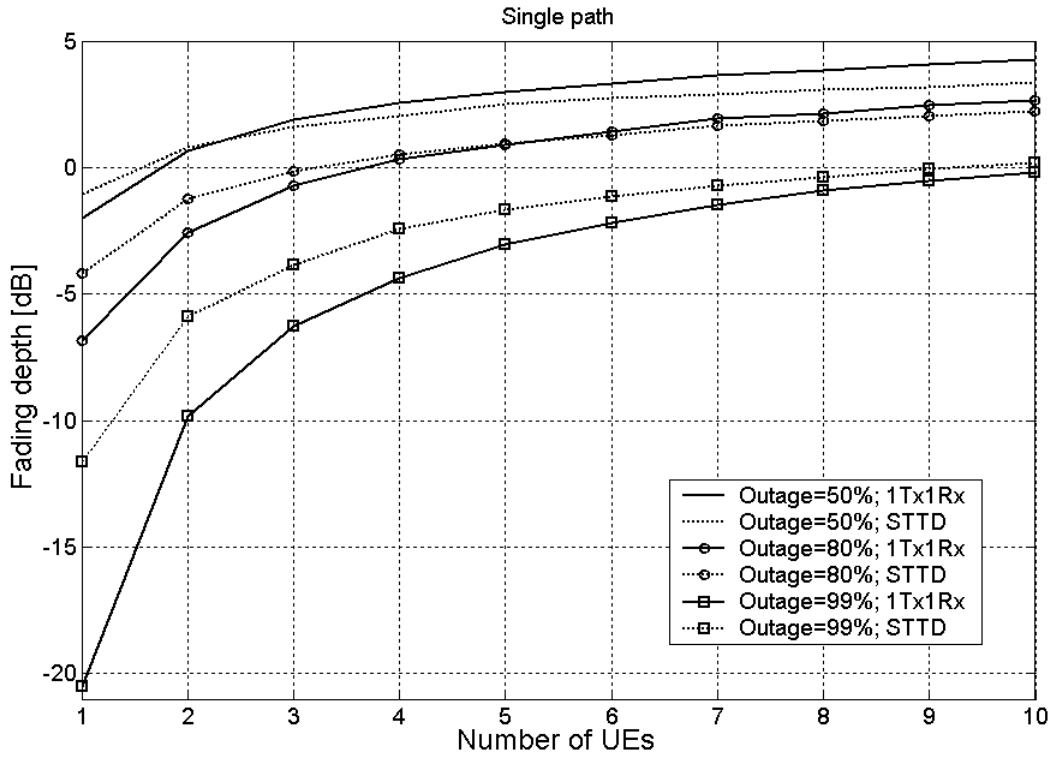

Figure 3.2 Fading depth at the shared channel for a single path propagation environment.

In Figure 3.3, the fading depth at the shared channel is plotted as a function of the number of UEs for a two-path channel. According to the results presented here, the gain from applying fast scheduling so that UEs are scheduled on the top of a fade is lower than in the single path channel. The reason for this is that a two-path channel already provides some diversity and, as a consequence, the channel amplitude on the top of constructive fades is statistically worse. Thus, scheduling UEs experiencing constructive fading does not bring so much gain.

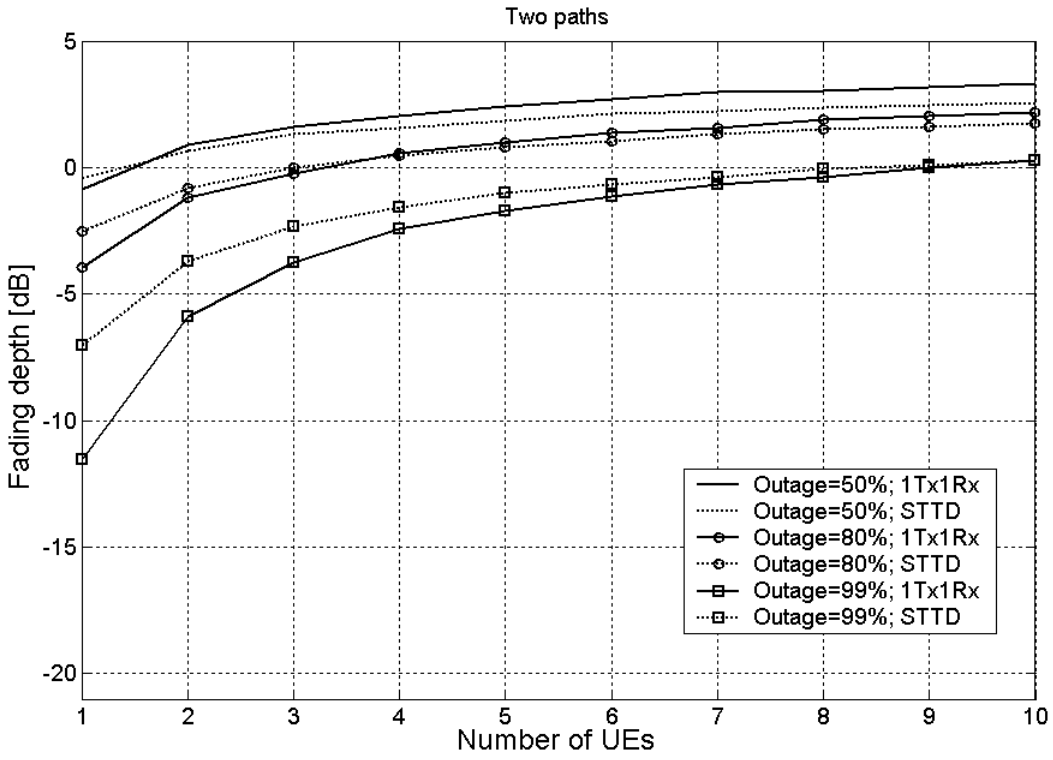

Figure 3.3 Fading depth at the shared channel for a two-path propagation environment.

However, these preliminary conclusions have been extracted assuming ideal instantaneous selection of the UE with the best instantaneous normalised channel quality. In practice, such operation is subject to delays. As a consequence, the conclusion of the analysis depends on the UE speed, since there are certain mechanisms that become more robust against delays (and thus against the UE speed) when STTD is enabled. Examples of such processes are the feedback procedures for the information required for link adaptation and fast, channel quality based packet scheduling.

For this simple theoretical discussion, the interaction between UE speed, antenna diversity and performance of fast channel quality based packet scheduling is analysed. The influence of link adaptation will be accounted for later by including the equivalent detailed model for the simulation campaigns.

Figure 3.4 concentrates on the case in which there are 10 UEs in the system, among which the packet scheduling algorithm selects the one with the best normalised channel quality. Unlike in the previous plots, now the system applies a delay of 4 ms (2TTIs in the HSDPA specifications), which elapses from the moment at which the selection of the best UE is done until the moment in which the result of such selection is applied.

As can be seen, at very low speeds, the single antenna solution yields better performance, due to the reasons already mentioned throughout this Section. However, as the UE speed increases, the single antenna performance degrades more than that of the STTD configuration.

As a consequence, there is a UE speed value from which the STTD option becomes better. The reason is that, although STTD stabilises the channel and smoothens the constructive fades, the experienced channel stabilization also makes the system less sensitive towards the delays in the scheduling decisions.

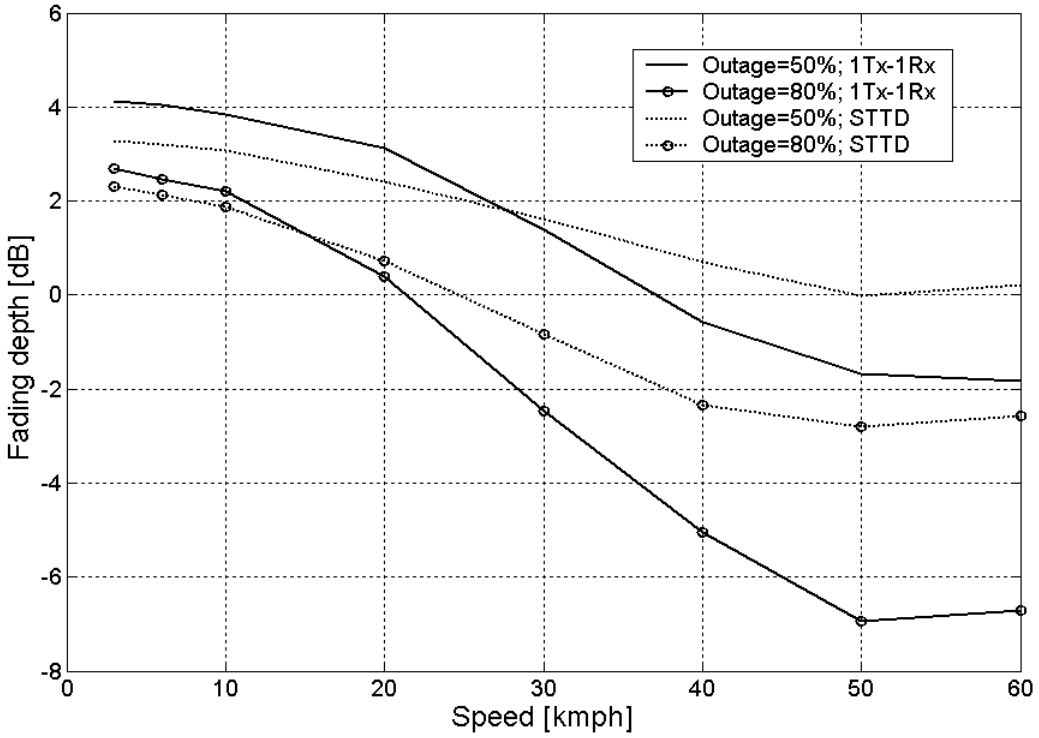

Figure 3.4 Fading depth at the shared channel for a single path propagation environment as a function of the UE speed. The scheduling decisions suffer from a delay of 4 ms.

3.2 System model

This subsection describes the system model and the simulation approach that have been used in order to generate the results that will be presented later.

3.2.1 Basic simulation methodology

The basic simulation methodology follows that of [17], where a standard hexagonal grid with 3-cell Node-B's is considered. The simulator is operated at slot level, using the so-called actual value interface (AVI) to model the link performance of the connection between each UE and its serving Node-B [12].

The deterministic path loss between each Node-B and each UE is calculated according to the single-slope model given by Okumura-Hata [13]:

$$PL(R) = A + B \cdot \log 10(\max\{0.05, R\}) \quad [dB], \tag{3.1}$$

where A equals –128.1 and B equals 10 times the propagation exponent, which has been set to the value of –3.5.

An independent fast fading process is simulated for each Node-B–UE pair. Within each Node-B–UE link, as many independent single-ray fading processes as the number of taps in the power delay profile (PDP) are simulated. The power value of the single-ray fading processes is Rayleigh distributed, and the complex value of the radio channel is also available, since it is required for the simulation of some advanced antenna schemes. For the total fading within one link, the power values of these processes are combined according to the corresponding power gain values in the PDP. Two modified PDPs are available for simulation: ITU Pedestrian A and ITU Vehicular A [14].

Shadow fading is assumed to be lognormal distributed. Given a certain Node-B, the shadow fading of the links between that Node-B and all the UEs in the system are completely independent. However, when two Node-B belong to the same site, they exhibit exactly the same shadow fading towards the UEs, i.e., for a given UE, the shadow fading towards those two Node-B is the same, although the values for different UEs is still independent.

UEs are connected to the cell with the smallest integral path loss, averaged over fast fading.

3.2.2 Model for the HSDPA concept

A fixed amount of transmit power and a fixed number of channelization codes are reserved for transmission of the high speed physical downlink shared channel (HS-PDSCH). The channelization codes for the HS-PDSCH use spreading factor 16. The remaining transmit power at the Node-B is assumed to be used by other channel types; so the Node-B transmit power is constant and identical for all cells in the simulated network.

A single UE is served in each transmission time interval (TTI) per cell. By means of a Link Adaptation (LA) algorithm, the optimum modulation and coding scheme (MCS) and the number of parallel channelization codes (multi-codes) are selected as a function of the instantaneous channel quality experienced by the served UE. Selection of the optimum MCS is based on the Channel Quality Indicator (CQI) report from the UE [16]. For the sake of simplicity, this study only considers the five MCSs listed in Table 3.1, although more options are allowed for the HSDPA concept. Possible LA algorithms for selection of optimum MCS are discussed in [18].

Table 3.1. Modulation and coding schemes.

Identifier	MCS #1	MCS #2	MCS #3	MCS #4	MCS #5
Modulation	QPSK	QPSK	16QAM	16QAM	16QAM
Effective code rate	1/4	1/2	3/4	1/2	3/4

Hybrid Automated Request (H-ARQ) is implemented in the simulator. Whenever a TTI is detected to be erroneous, a fast layer 1 retransmission process is started. After a certain delay (specified as a parameter), the TTI is retransmitted with the same number of multi-codes and the same MCS. Then, the soft samples of the received retransmission are soft combined with the ones of the faulty transmission. If successful decoding of the result is possible, the process is finished here. If not, another retransmission process is started, and the soft samples of all the retransmissions are combined. In practice, there is a maximum number of retransmissions, after which the buffer containing the accumulated soft samples is flushed and the link adaptation process is started all over again for the same data. In the simulator used for this study, maximal ratio combining is used to combine the soft samples of the retransmissions with the ones already stored in the buffer. This choice is often referred to as Chase Combining, although there are other possibilities. The combining loss for all the possible schemes is studied in [15], and the guidelines given here are adopted to model the performance of Chase Combining in this study.

Since there is a minimum delay between retransmissions, a stop and wait (SAW) procedure has been implemented in order to be able to continue the transmission towards a certain UE even though one of the TTIs is waiting for a retransmission whose time has not come yet. The number of SAW channels is dimensioned accordingly to the delay between retransmissions, so that the communication towards the UE is not halted because of the delays in the retransmissions.

Moreover, no matter the selected packet scheduling strategy, whenever there is a retransmission ready to be sent, it is allocated higher priority than the decision of the packet scheduler. The danger of getting the system blocked by continuous retransmissions coming from an unfortunate LA operation is avoided by setting a maximum number of retransmissions.

3.2.3 Link level performance model

This subsection focuses on the way in which the antenna schemes are modelled when conducting the interference calculations in the network simulator. Before starting this description, some general comments and guidelines are given, regarding general modelling strategies and notation issues.

The simulations applying the models that are going to be described below are run with a time resolution of one slot, and the basic modelling effort is concentrated on calculating the E_S/N_0 that is experienced at the HS-PDSCH at a certain slot.

As already mentioned, the detection of the signals is modelled using the so-called AVI principle [12]. Prior to explaining the basics of this principle, let us define a transport block as a set of slots that are decoded all together. In the case of the HS-PDSCH, this block is a transmission time interval (TTI), comprising three slots. With the AVI method, whenever a set of slots completing a transport block has been received, the equivalent E_S/N_0 of the block is computed as the geometrical average of the E_S/N_0's of all the slots in the block. Then, a lookup table (generated from extensive link level simulations, according to the HSDPA specifications [3]) maps the block E_S/N_0 to an equivalent Block Error Probability (BEP). A

uniform distributed number ($\chi \in [0;1]$) is generated and compared to the BEP. If χ < BEP, the block is labelled as erroneous. Otherwise, it is labelled good. Different AVI tables are used depending on the MCS that is used for transmission towards the UE. Moreover, when applying this model to the reception of a HS-PDSCH transmitted on several multi-codes, a lookup table generated for one single code is used, and the input value that is fed into this table equals the geometrically averaged E_S/N_0 divided into the number of used multi-codes. The result of this look-up is then taken for all the used multi-codes. The gain from combining re-transmissions is modelled according to [15], assuming that Chase Combining is used.
The calculation process of the E_S/N_0 takes the effect from multi-path propagation into account (including the so-called downlink orthogonality) and the potential gain from using transmit/receive antenna diversity. The expressions for the per-slot E_S/N_0 are reported in the following subsections, using the notation in Table 3.2. Note that in deriving these expressions it has been implicitly assumed that a standard Rake receiver with maximal ratio rake finger combining is used at the UE. Furthermore, it has been assumed that the Node-B antennas and UE antennas are uncorrelated, with equal branch power ratio.

Table 3.2. Notation for the relevant magnitudes in the interference calculation.

Symbol	Definition
L	Number of multipath components tracked by the Rake receiver associated to one antenna. Perfect maximal ration combining between them is assumed.
P	Number of multipath components in the considered power-delay spectrum.
SF	Spreading factor.
N	Power for the thermal noise at the UE.
B	Number of Node-B's in the network.
S	Number of the serving Node-B.
P_i	Signal power transmitted towards UE number i on the HS-PDSCH at the current slot.
P_b^{Total}	Total wideband transmitted power from Node-B number b.
$h_L(b, i)$	Shadow faded path loss from Node-B number b to UE number i.
$h_{FF,t}^{r}(b, i, l)$	Power gain of the fast fading multipath component number l of the link between the t^{th} transmit diversity branch of Node-B number b and the r^{th} receive diversity branch of UE number i.
$f_{FF,t}^{r}(b, i, l)$	Complex gain value of the fast fading multipath component number l of the link between the t^{th} transmit diversity branch of Node-B number b and the r^{th} receive diversity branch of UE number i.
a	Serving Node-B
w_k	Transmission weight for the k^{th} transmit diversity branch in CLTD.

Model for 1Tx-1Rx

For single antenna at both the Node-B and the UE (1Tx-1Rx), the E_S/N_0 is modelled as:

$$\frac{E_S}{N_0}(i)=\sum_{l=1}^{L}\frac{SF\cdot P_i h_L(a,i)h^1_{FF,1}(a,i,l)}{N+\sum_{b=1}^{B}\sum_{d=1}^{D}P_b^{Total}h_L(b,i)h^1_{FF,1}(b,i,d)-P_a^{Total}h_L(a,i)h^1_{FF,1}(a,i,l)} \tag{3.2}$$

Model for STTD

$$\frac{E_S}{N_0}(i)=\sum_{l=1}^{L}\frac{SF\cdot P_i\cdot\frac{h_L(a,i)}{2}\left(h^1_{FF,1}(a,i,l)+h^1_{FF,2}(a,i,l)\right)}{N+\sum_{b=1}^{B}\sum_{d=1}^{D}P_b^{Total}h_L(b,i)\frac{1}{2}\begin{pmatrix}h^1_{FF,1}(b,i,d)+...\\ ...h^1_{FF,2}(b,i,d)\end{pmatrix}-P_a^{Total}h_L(a,i)\frac{1}{2}\begin{pmatrix}h^1_{FF,1}(a,i,l)+...\\ ...h^1_{FF,2}(a,i,l)\end{pmatrix}} \tag{3.3}$$

Model for CLTD

$$\frac{E_S}{N_0}(i)=\sum_{l=1}^{L}\frac{SF\cdot P_i h_L(a,i)\left\|w_1 f^1_{FF,1}(a,i,l)+w_2 f^1_{FF,2}(a,i,l)\right\|^2}{N+\sum_{b=1}^{B}\sum_{d=1}^{D}P_b^{Total}h_L(b,i)\frac{1}{2}\begin{pmatrix}h^1_{FF,1}(b,i,d)+...\\ ...h^1_{FF,2}(b,i,d)\end{pmatrix}-P_a^{Total}h_L(a,i)\frac{1}{2}\begin{pmatrix}h^1_{FF,1}(a,i,l)+...\\ h^1_{FF,2}(a,i,l)\end{pmatrix}} \tag{3.4}$$

Model for 2Rake

$$\frac{E_S}{N_0}(i)=\sum_{r=1}^{2}\sum_{l=1}^{L}\frac{SF\cdot P_i h_L(a,i)h^r_{FF}(a,i,l)}{N+\sum_{b=1}^{B}\sum_{d=1}^{D}P_b^{Total}h_L(b,i)h^r_{FF,1}(b,i,d)-P_a^{Total}h_L(a,i)h^r_{FF,1}(a,i,l)} \tag{3.5}$$

Model for CLTD+2Rake

For CLTD at the Node-B and the 2Rake at the UE (CLTD+2Rake), the E_S/N_0 is modelled as:

$$\frac{E_S}{N_0}(i)=\sum_{r=1}^{2}\sum_{l=1}^{L}\frac{SF\cdot P_i h_L(a,i)\left\|w_1 f^r_{FF,1}(a,i,l)+w_2 f^r_{FF,2}(a,i,l)\right\|^2}{N+...\quad\sum_{b=1}^{B}\sum_{d=1}^{D}P_b^{Total}h_L(b,i)\frac{1}{2}\begin{pmatrix}h^r_{FF,1}(b,i,d)+...\\ ...h^r_{FF,2}(b,i,d)\end{pmatrix}-P_a^{Total}h_L(a,i)\frac{1}{2}\begin{pmatrix}h^r_{FF,1}(a,i,l)+...\\ h^r_{FF,2}(a,i,l)\end{pmatrix}} \tag{3.6}$$

3.2.4 Packet scheduling

In this Section, the three basic packet scheduling strategies considered for this study are presented. These schedulers do not include any kind of advanced flexible quality of service awareness, which should be of course included in the real system in order to be able to tailor

the offered service to the given requirements. Therefore, the algorithms presented here must be taken just as basic reference cases, which are useful to benchmark the performance of the different antenna configurations, and identify the different mechanisms that govern the interaction between antenna diversity and packet scheduling. For this study, it is assumed that the packet scheduler selects the UE to be served on a TTI basis.

Round Robin

In the considered Round Robin (RR) algorithm, the UEs are served in sequential order. Hence, the scheduling is conducted blindly without using any a priori knowledge of the state of the radio channel, which results in a relatively large variance in the average data rates among the UEs in the cell [19]. This algorithm provides all the UEs with the same network resources, which does not mean that all of them obtain the same quality of service, since each of them experiences different channel quality.

Fair Throughput

As stated before, the use of RR results in better throughput for those UEs in good radio channel conditions, while those UEs with a poor radio channel typically obtain very small throughput. In order to overcome this lack of fairness, the fair throughput (FT) approach aims at delivering the same throughput to all the UEs in the cell. This can be done by, on a TTI basis, serving the UE with lowest throughput. In this way, the system converges to a situation in which all the UEs are given the same throughput, approximately. With this scheduler, the fairness is obtained at the expense of allocating more resources to those UEs with a poor radio channel, which leads to lower system throughput.

Proportional Fair

If fast information of the radio channel can be utilised, the scheduling can be done in such a way that the system performance is further optimised. This can be done in HSDPA because the packet scheduler is located in the Node-B, thereby enabling the system for fast scheduling. An obvious manner to maximise the global system throughput would be to serve the UEs with the best instantaneous radio channel conditions. This strategy is often referred to as maximum-C/I scheduling, where C/I stands for carrier-to-interference ratio, i.e., a way of measuring the instantaneous quality of the radio channel. However, although this strategy certainly maximises the system throughput, it is extremely unfair, which makes it less attractive from a service provider point of view.

In order to compensate for the lack of fairness when using the maximum-C/I scheduling while still taking advantage of the fast information of the radio channel, a proportional fair (PF) algorithm is considered instead. This algorithm aims at distributing the capacity among the UEs so the proportional fair equilibrium is reached. The proportional fair equilibrium is reached if an increase of X percent in throughput of any UE results in a total loss of more than X percent of the total throughput of the remaining UEs [9].

The algorithm selects the UE to be served in every TTI, according to a priority measure for each UE, which is expressed as [8]

$$A_i = \frac{R_i}{T_i}, \tag{3.7}$$

for UE number i, where R_i is the number of bits that UE number i can receive during the next TTI and T_i is the average throughput for the UE (also called the monitored throughput). The UE with the highest priority is served. This approach provides an appealing throughput levelling mechanism by introducing a trade-off between cell throughput and fairness.

The average throughput, T_i, for each user is computed as the total number of bits transmitted to that user, divided by the time-period where there have been bits to transmit to that particular user. Computation of T_i might also be limited to a certain observation window of Di seconds, so that only the recent history is used when calculating T_i and therefore also the priority metric in (3.7). As discussed in [10], adjustment of Di provides an efficient mean of partly controlling the maximum delay allowed for the different users. This can be exemplified as follows: Provided that no data have been transmitted to user i for a time period longer than Di, then T_i=0, which results in Ai$\rightarrow\infty$ (i.e., the user is served immediately). Application of different window functions is discussed in [10], such as rectangular windows, windows with exponential decays, etc. For the sake of simplicity, a rectangular window shape with infinite size will be assumed in the sequel.

Basically, after the initial convergence mechanisms have stabilised, this scheduler attempts to schedule UEs when they are experiencing constructive fading, i.e., the selection metric is defined in such a way that the UE with maximum instantaneous normalised channel quality is selected. The aforementioned normalised instantaneous quality measure appears projected into the throughput dimension, in order to account for the non-linearity between E_S/N_0 and throughput caused by the use of higher order modulation schemes [11]. As a consequence, provided that all the UEs enjoy the same dynamic range, this scheduler provides a fair distribution of resources among the UEs. Moreover, the system performance is enhanced by the fact that they are served when they experiencing constructive fading, which results in the so-called multi-user diversity gain [19].

3.2.5 Admission control

Whenever an HSDPA UE is generated, it can be admitted or blocked, depending on whether there is room for it in the service queue. Thus, the admission control criterion is very simple. Let N be the number of UEs already being served in the system. Then, a new UE can be admitted in the system if

$$N < N_{MAX}\,, \tag{3.8}$$

where N_{MAX} is set as a simulation parameter.

3.2.6 Measurement errors and feedback delays

The LA process, the reporting of CLTD weights and the operation of the proportional fair packet scheduling algorithm rely on measured information of the instantaneous radio channel experienced by the UEs. For LA and packet scheduling, this information is included in the CQI reports sent by the UEs, while in CLTD the UE estimates the optimum transmission weights and feeds them back to the Node-B. The following describes the way in which the impairments affecting these mechanisms are modelled in the simulator.

For the generation of the CQI, a simple model for the estimation errors is applied. This model assumes a lognormal distributed error on the equivalent E_S/N_0 estimate, before mapping to CQI. Similarly, the channel estimate for calculation of the optimum CLTD weight (one of four possible phase values) is also assumed to include a lognormal distributed channel estimation error. The standard deviation of the error for both CQI reports and derivation of the CLTD weight is assumed to equal 1dB.

Signalling delays for reporting of CLTD weights and CQI reports from the UEs are also included in the simulator. The delay figures must be interpreted in the following way:

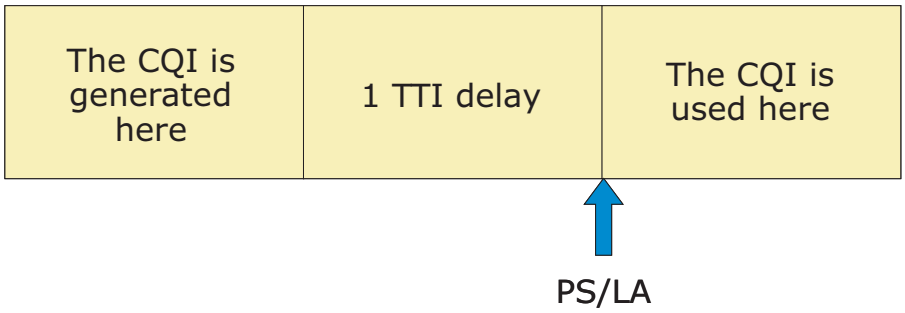

Figure 3.5 Example of CQI delay = 1 TTI.

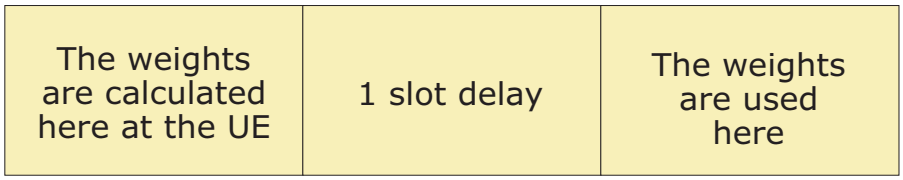

Figure 3.6 Example of CLTD delay = 1 slot.

The uplink channel is also subject to detection errors, which affect the transmission of the selected weights for CLTD. This effect is modelled by an uplink command error probability. For each use of the uplink command, a random number between 0 and 1 is generated. If the number is below the error probability, the command is assumed to be erroneous and the actions for the wrong uplink command information are triggered. These actions can consist of a wrong update in the weights for CLTD. When an error is made in the transmission of the CLTD weights, the wrong set of coefficients is applied. In this respect, it has to be pointed out that the UE is assumed to be able to conduct perfect antenna verification [16]. This means that, even though the wrong weights are applied, the UE is able to determine which weights were applied at the Node-B by comparing the dedicated pilot from the second antenna and the common pilot. Thanks to perfect antenna verification, the UE is always assumed to be able to estimate the radio channel and receive the signals. Of course, if there has been an error applying the weights, the received E_S/N_0 is lower, which results in a larger error probability.

3.2.7 Traffic modelling

A single payload model is adopted for the amount of data in the Node-B for each UE, and a Poisson distributed call generation process is simulated. Whenever a new call is generated, the UE position is selected randomly in the network. Each call is assumed to consist of 100 kbits,

which have to be transmitted to the UE. When the payload is successfully transmitted, the call is terminated.

The simulator offers the possibility to drop those UEs that do not fulfil certain minimum requirements regarding quality of service. In this context, the dropping criterion is very simple: after the UE has been in the system for a number of periods larger than T_{min}, if the overall packet call throughput falls below a certain minimum R_{min} the UE is dropped. By default, T_{min} and R_{min} are set to 10 seconds and 10kbps, respectively.

3.2.8 Default simulation parameters

Table 3.3 summarizes the default simulation parameters. At this point, it is convenient to show the G factor distribution collected for the proposed set of parameters and simulation assumptions. Note that the G factor is computed according to the guidelines given in [3].

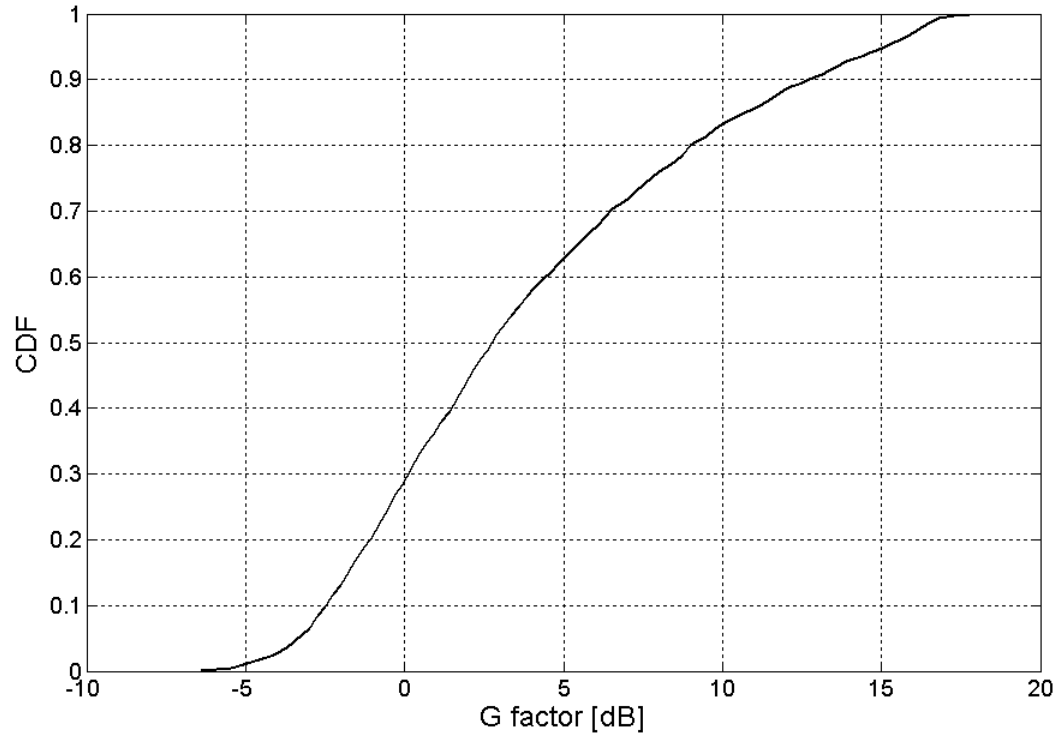

Figure 3.7 G factor distribution for the proposed set of parameters and simulation assumptions.

Table 3.3. Default simulation parameters.

Parameter	Value
Propagation environment	Urban macro cell

Distance between sites	2000 m
Power-delay profile of the radio channel	ITU Pedestrian A
Std of shadow fading	6 dB
UE speed	3 kmph
Max. transmit power at the Node-B	20 W
Power for the HS-PDSCH	9 W
Number of codes for the HS-PDSCH	7
Max. number of queued UEs in the cell	32
Offered load	3 Mbps
Payload of each UE	100 kbits
Method for retransmissions	Chase combining. Modelled.
Priority for retransmissions	High
Delay for retransmissions	6 TTIs
Max number of retransmissions	6
Number of SAW channels	6
LA delay	2 TTIs
PS delay	2 TTIs
Delay for CLTD	2 slots
Error probability of the uplink feedback	4%

3.3 Simulation results

This subsection begins by showing the HSDPA cell pole capacity for Pedestrian A at 3 kmph, under all the considered antenna schemes and packet scheduling strategies. Note that the pole capacity is reached when the offered load is significantly above the system capacity, i.e., when the blocking rate is very high. Based on these results, some conclusions are extracted about the main performance differences between the three selected schedulers for the single antenna case. These explanations serve as a starting point for the discussion on how the system performance evolves when the antenna diversity techniques under study are deployed.

After describing the gain that the advanced antenna diversity schemes can provide in terms of system throughput, an analysis is conducted on how the aforementioned throughput gain affects the different UEs in the system, depending on their G factor. Afterwards, further analysis items are addressed in order to assess the dependency of the system performance on the multipath propagation environment, the queue size and the UE speed.

After analysing the system performance and the impact of all the aforementioned effects in a situation with very high blocking probability (i.e. concerning the pole system capacity), the basic case (Pedestrian A at 3 kmph) is selected for a more detailed analysis, in which the outage (defined as the proportion of UEs that are dropped, blocked or obtain less than a certain throughput value) is included as an extra dimension.

3.3.1 Results for Pedestrian A and 3 kmph

The HSDPA cell pole capacity achieved for the different simulation options is summarized in Table 3.4. Note that the total cell capacity is larger than the reported HSDPA cell capacity, since only a fraction of the cell resources (power and codes) are allocated to HSDPA.

Table 3.4. Results for Pedestrian A and 3 kmph.

Scheme	RR			PF			FT		
	HSDPA cell capacity [Mbps]	Gain compared to 1Tx-1Rx	Gain compared to RR	HSDPA cell capacity [Mbps]	Gain compared to 1Tx-1Rx	Gain compared to RR	HSDPA cell capacity [Mbps]	Gain compared to 1Tx-1Rx	Gain compared to RR
1Tx-1Rx	0.944	0%	0%	1.789	0%	90%	0.648	0%	-31%
STTD	1.063	13%	0%	1.662	-7%	56%	0.876	35%	-18%
CLTD	1.378	46%	0%	2.003	12%	45%	1.187	83%	-14%
2Rake	1.722	82%	0%	2.313	29%	34%	1.485	129%	-14%
CLTD+2 Rake	2.106	123%	0%	2.471	38%	17%	1.949	201%	-7%

3.3.2 1Tx-1Rx: Influence of the packet scheduling algorithm

As can be seen in Table 3.4, the scheduler yielding the highest system throughput for the 1Tx-1Rx case is PF, due to the fact that this scheduler takes advantage of fast information about the state of the radio channel. In fact, PF gives a system throughput gain of 90%, compared to RR. On the other side of the spectrum, FT is the one providing the lowest system throughput, giving a loss of 31% compared to RR. The reason is that many resources are allocated to UEs in poor channel conditions in order to provide the same throughput over the entire cell.

This phenomenon is illustrated in Figure 3.8, which shows the average UE throughput as a function of the G factor. As it can be seen, FT provides the same throughput for all the UEs, even for those with very low G factors, whereas RR does not assign so many resources to those UEs and, in return, gives better throughput to the rest of the UEs. For UEs with very low G factors, PF still provides the same throughput as FT without seriously jeopardizing the system performance. This is possible because PF uses fast information about the state of the radio channel in order to schedule the UEs when they experience constructive fading.

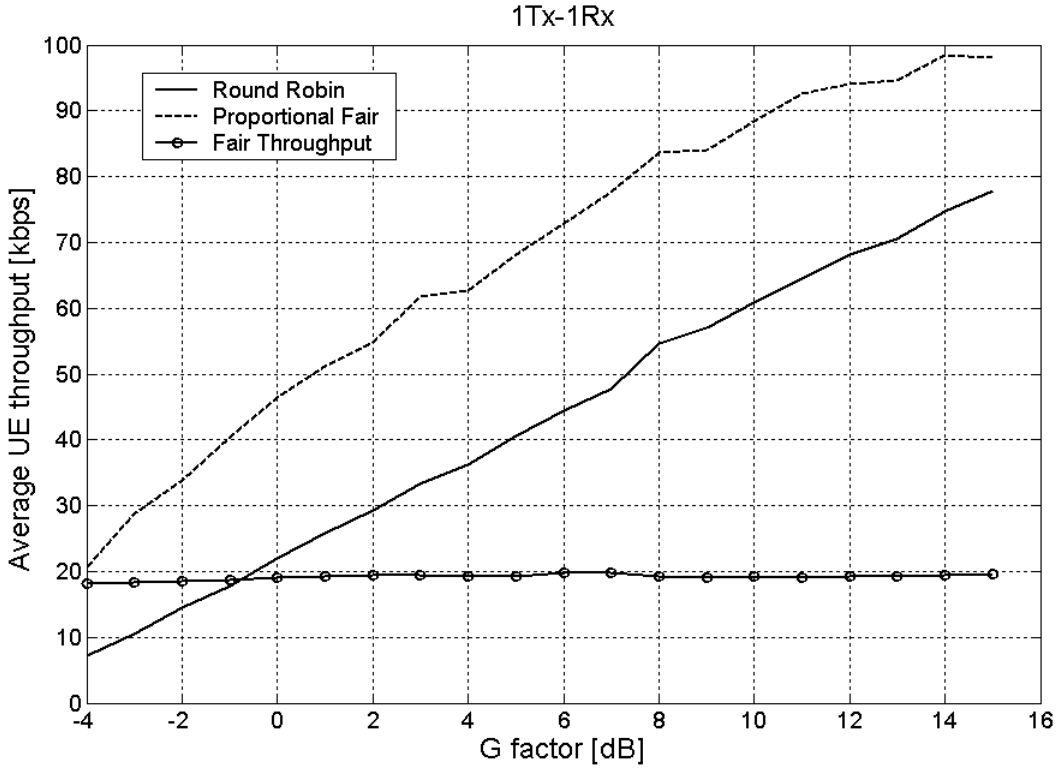

Figure 3.8 Average UE throughput vs. G factor.

In PF, due to the large experienced E_S/N_0's, the probability of selecting higher MCS is larger. On the other hand, FT focuses the resources on poor UEs. Thus, the probability of selecting higher MCS in the network is lower. This is illustrated in Figure 3.9, which shows the MCS selection probability and a histogram of the number of multi-codes for 1Tx-1Rx with the three packet scheduling algorithms under study.

3.3.3 Capacity gain from transmit and receive diversity

STTD

When STTD is enabled with RR schedulers, a system throughput gain of 13% is experienced, while a loss of 7% can be seen for PF. In the case of FT, the achieved gain equals 35%.

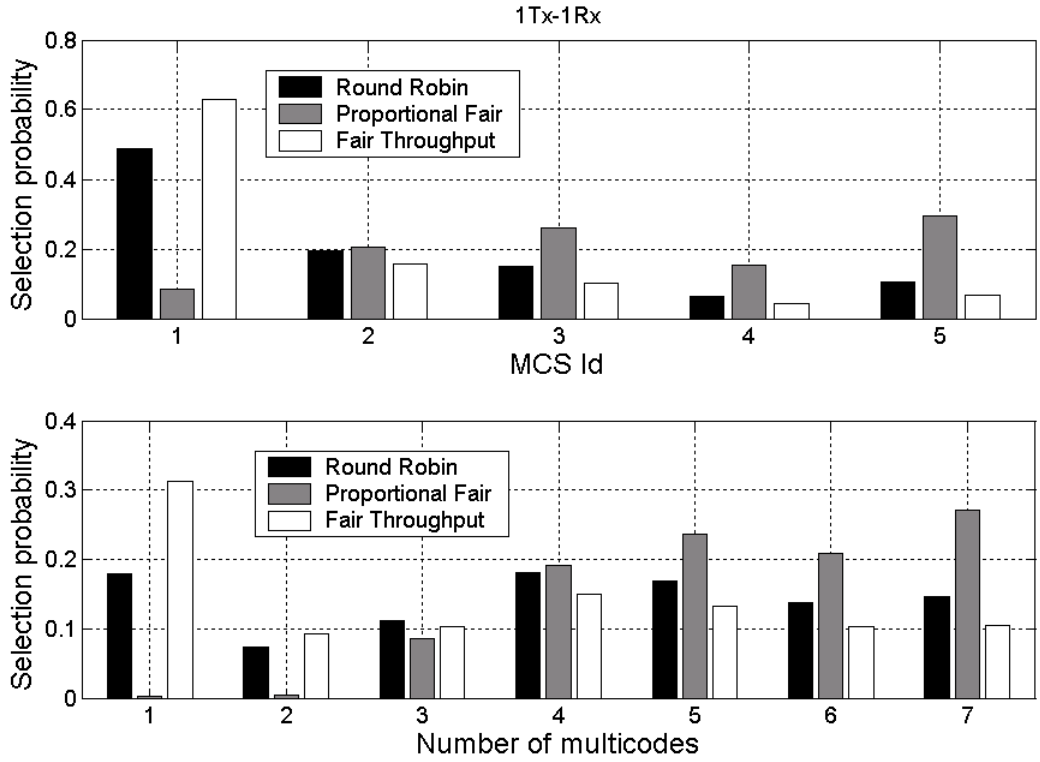

Figure 3.9 MCS selection probability for 1Tx-1Rx. Pedestrian A.

The reason why STTD yields a loss in PF was already presented in Subsection 3.1, and this result is in line with the study described in [7] [20]. In short, it can be said that PF aims at scheduling the UEs when they are experiencing constructive fading. Moreover, it is known that the channel quality on the top of a constructive fade is statistically worse when the radio channel is stabilised, e.g. by the use of STTD. Other schedulers, such as RR and FT, serve UEs no matter what their channel quality is and, thus, benefit from the suppression of deep fades provided by STTD, and this is the reason why they experience a capacity gain. This is not the case for PF, where the scheduler avoids transmission during deep fades.

Moreover, STTD yields more capacity gain in FT than in RR due to two reasons. On one hand, FT puts more resources on UEs under poor channel conditions. As shown in Figure 3.9, this implies less frequent use of 16QAM, which allows for translation of the E_S/N_0 improvements into higher data rates primarily by using more multi-codes for transmission or a lower effective coding rate. This strategy is more spectral efficient than using higher order modulations [11], and implies an approximately linear relationship between the E_S/N_0 improvement and the increase of the UE data rate. However, when the capacity figures are higher in the 1Tx-1Rx case, exploitation of the E_S/N_0 improvement by using higher order

modulations becomes more frequent and lower increases of the UE data rates are experienced for an equivalent E_S/N_0 improvement.

On the other hand, the UEs far away from the Node-B, which are the ones receiving most resources from the FT scheduler, receive a larger fraction of interference from other cells. Under these circumstances, stabilisation of the radio channel via STTD has a strong impact on stabilisation of the E_S/N_0. However, for UEs near the Node-B, most of the interference is coming from the same Node-B that transmits the desired signal. This provides implicit stabilisation of the E_S/N_0 for the 1Tx-1Rx case, since both signal and interference are fading with the same pattern. Therefore, for UEs near the serving Node-B, the more stable nature of the E_S/N_0 makes it more difficult to benefit from the diversity protection provided by STTD. As a consequence, since FT assigns more resources to UEs far away from the serving Node-B, it allows for a better improvement in the experienced E_S/N_0, which is translated into a better throughput gain.

Figure 3.10 shows the distribution of the received E_S/N_0 at the shared channel, including the values from all the served UEs. As can be seen, the usage of STTD with PF does indeed degrade the E_S/N_0 of the received signals. Moreover, it can be also noticed that the largest E_S/N_0 improvement due to diversity is experienced for FT, due to the aforementioned reasons. Furthermore, another phenomenon that can be confirmed in these plots is that PF yields the largest E_S/N_0 values, due to the fact that it schedules UEs when they are on the top of a constructive fade.

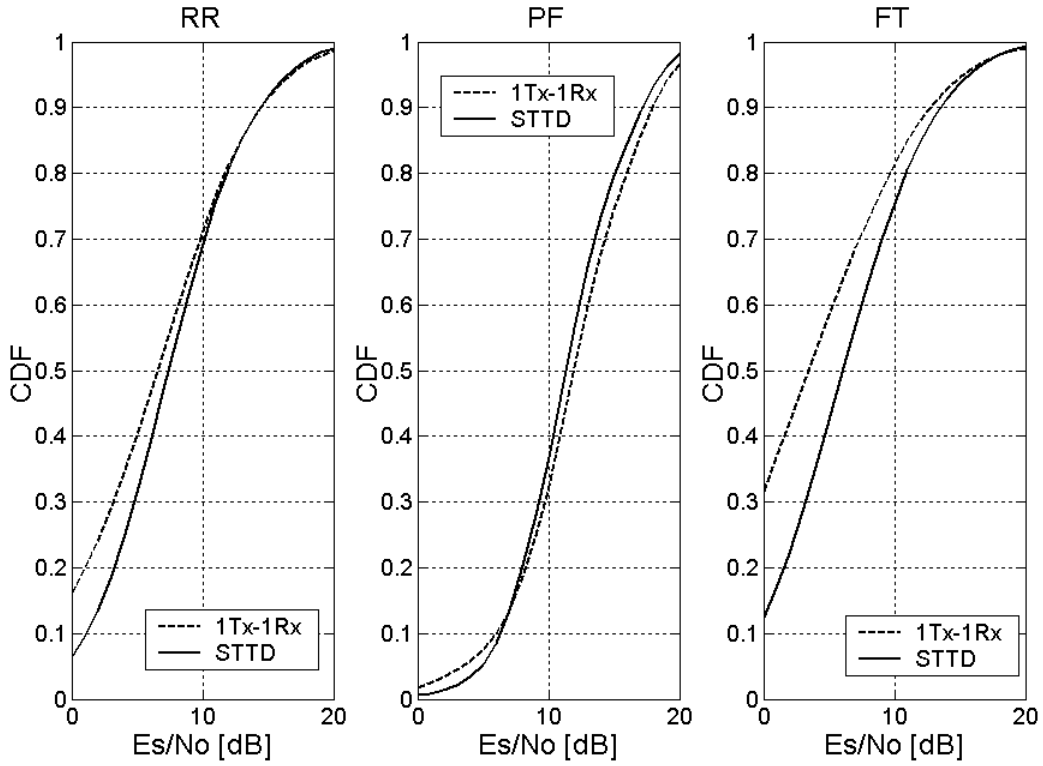

Figure 3.10 E_S/N_0 distribution at the HS-DSCH.

Notice however that, in spite of the throughput loss that PF experiences when STTD is enabled, it is still the scheduler with the largest absolute system throughput. Compared with 1Tx-1Rx, the gain of going from RR to PF drops from 90% to 56% when STTD is implemented. Furthermore, when enabling STTD, the loss due to going from RR to FT drops from 31% to 18%.

2Rake

When 2Rake receivers are implemented, the received E_S/N_0 at the UEs is affected in two ways: (i) on one hand, an average E_S/N_0 improvement of 3dB is experienced; and (ii), the diversity protection of the signals is increased, i.e., the radio channel is stabilised.

This can be seen in Figure 3.11, which plots the distribution of the received E_S/N_0 at the shared channel, including the values from all the served UEs. As can be seen in the picture, the overall E_S/N_0 improvement is larger than 3dB for both RR and FT, since this improvement comprises both the average gain and the diversity protection. Moreover, it can be observed that this improvement is larger for FT, due to the mechanisms already described for STTD. On the other hand, since the diversity protection provides a loss in PF, the overall E_S/N_0 improvement with this scheduler is smaller than 3dB, accounting for the 3dB combining gain and the loss from stabilising the radio channel while using PF.

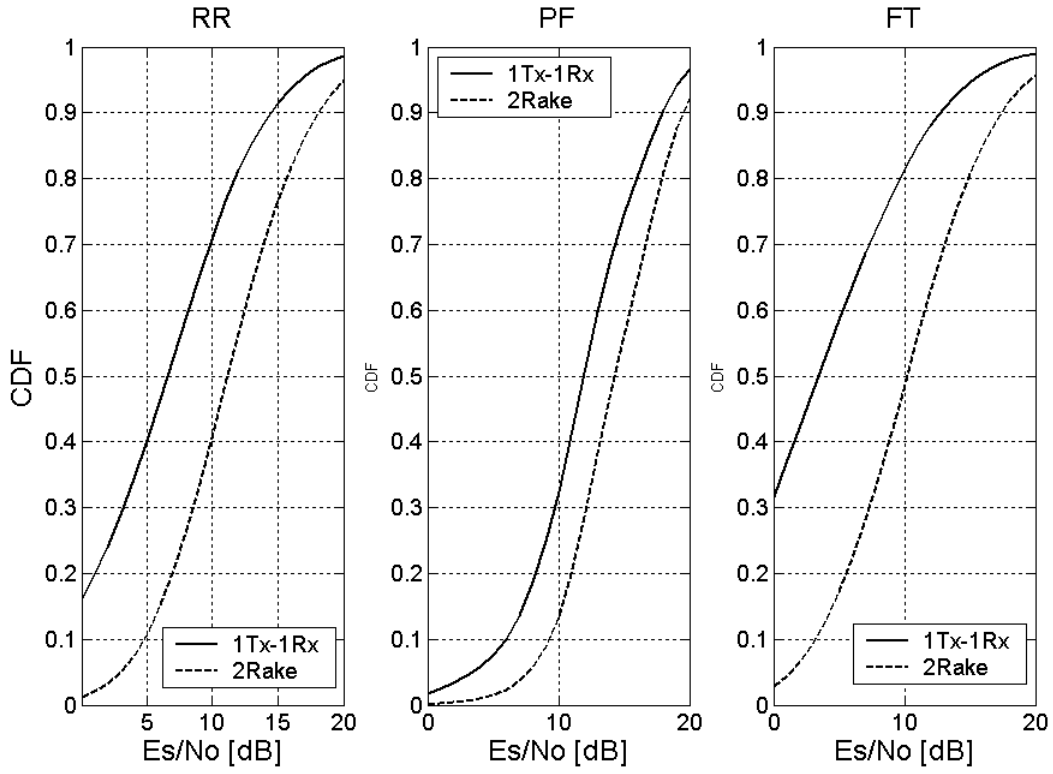

Figure 3.11 E_S/N_0 distribution at the HS-DSCH.

Thus, it can be seen that the scheme for which the deployment of 2Rake receivers provides the largest E_S/N_0 improvement is FT. On the other hand, the lowest E_S/N_0 gain is experienced

for PF. Furthermore, as already shown in Figure 3.9, FT is the scheduler for which the 1Tx-1Rx scheme uses the lowest MCS, which implies that it is also the scheme that can map the E_S/N_0 gain into throughput gain in a more efficient manner. On the other hand, PF is the scheduler using the highest MCS for the 1Tx-1Rx, and it can therefore exploit the E_S/N_0 gain in a less spectral efficient fashion.

The two aforementioned phenomena justify the fact that the deployment of 2Rake receivers yields the highest throughput gain in FT (129%), while it provides the lowest throughput increase in PF (29%). The throughput gain figures for RR lay in the middle (82%). Again, in spite of the lower throughput gain that PF experiences when 2Rake receivers are deployed, PF is still the scheduler with the largest absolute system throughput. Nevertheless, compared with the 1Tx-1Rx case, the gain of going from RR to PF drops from 90% to 34%, while the loss due to going from RR to FT drops from 31% to 14% when STTD is implemented.

Figure 3.12 illustrates how the MCS selection probability evolves when 2Rake receivers are deployed under the packet scheduling strategies under study. As it can be seen, the information shown in this plot is in line with the trends shown in this discussion.

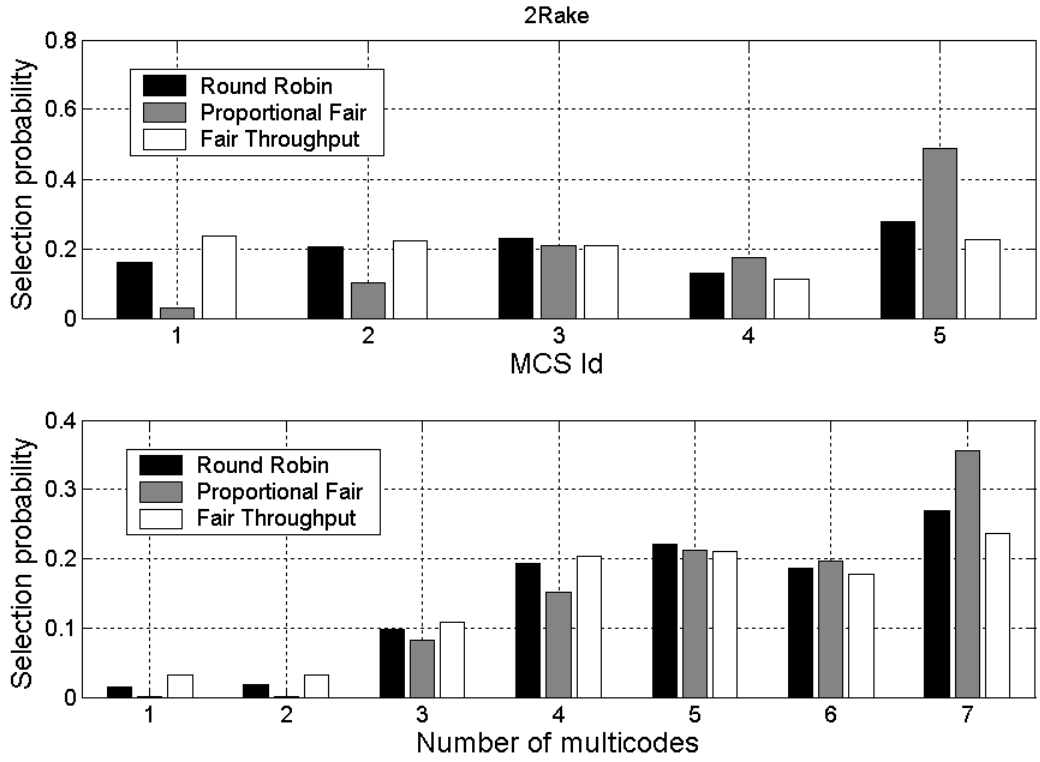

Figure 3.12 MCS selection probability for 2Rake. Pedestrian A.

CLTD

Like in the case of 2Rake, the deployment of CLTD provides both an average E_S/N_0 improvement and an extra diversity protection. However, the average E_S/N_0 gain is lower than that of 2Rake (3dB) due to several reasons:

- The selected CLTD scheme corresponds with the so-called Mode 1 of the UMTS specifications [16]. This means that there is a very coarse quantisation (in steps of 90°) for the calculation of the antenna weights. Moreover, no amplitude weighting between the antennas is allowed. As a consequence of the two aforementioned reasons, the performance of the CLTD scheme is worse than that of an ideal pre-MRC scheme, which should perform as the 2Rake scheme.
- The feedback information is not transmitted in an ideal manner. In fact, the information is delayed due to the processing and transmission time. In addition, the uplink control channel that carries the weights is not error free.
- The channel estimates that are used for the calculation of the optimum set of weights are polluted with a random estimation error, as described in Subsection 3.2.6.
- Even though the ITU Pedestrian A PDP is near the flat fading (single path) case, there are some small differences between them. Due to these differences, there are not enough degrees of freedom to fully adapt the transmission to the instantaneous state of all the multipath components in Pedestrian A.

The impact of all these phenomena on the achieved E_S/N_0 can be seen in Figure 3.13, which shows the distribution of the received E_S/N_0 at the shared channel, including the values from all the served UEs. For the sake of an easy comparison, the results for 2Rake are also included.

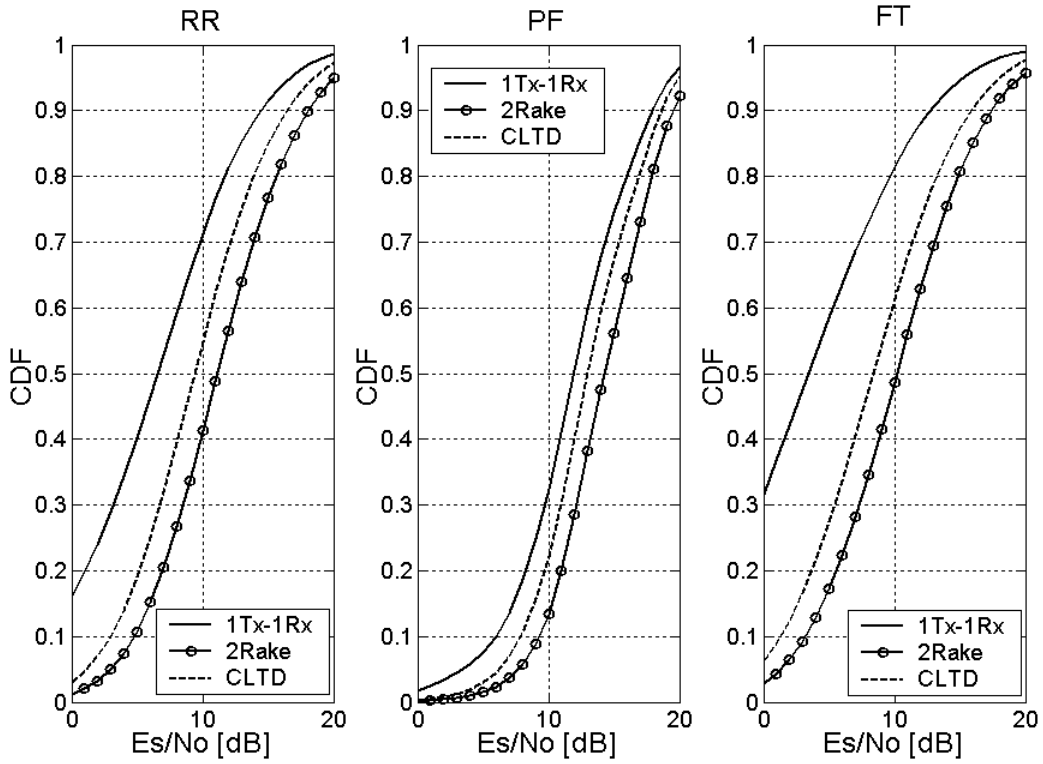

Figure 3.13 E_S/N_0 distribution at the HS-DSCH.

As can be seen, the results depicted in Figure 3.13 suggest that CLTD provides a lower average E_S/N_0 gain, although it still provides the same diversity protection that was experienced for 2Rake. The latter is inferred from the fact that the curves for both CLTD and 2Rake have the same slope, being one just a shifted version of the other.

As a consequence of the lower average E_S/N_0 gain, the achieved throughput increase is also lower. However, the same trends observed for the 2Rake case are still preserved here. The largest gain is experienced for FT (83%, while it was 129% for 2Rake), and the lowest one corresponds again to PF (12%, while it was 29% for 2Rake). Again, the value for RR lays in between the two other figures (46%, while it was 82% for 2Rake).

One more time, in spite of the lower throughput gain that PF experiences when CLTD is activated, PF is still the scheduler with the largest absolute system throughput. Nevertheless, compared with the 1Tx-1Rx case, the gain of going from RR to PF drops from 90% to 45%, while the loss due to going from RR to FT drops from 31% to 14% when CLTD is implemented.

CLTD+2Rake

The combination of CLTD and 2Rake involves the influence of all the mechanisms and phenomena that have been addressed when discussing each one of them on an individual basis. However, it is well known that, when two sources of diversity are combined, the resulting gain is lower than just the combination of the two individual gains. Therefore, the E_S/N_0 improvement for CLTD+2Rake is lower than the addition (in decibels) of the E_S/N_0 gain from CLTD and the E_S/N_0 gain from 2Rake receivers. This can be observed in Figure 3.14, where the E_S/N_0 distributions for 1Tx-1RX, CLTD, 2Rake and CLTD+2Rake are depicted.

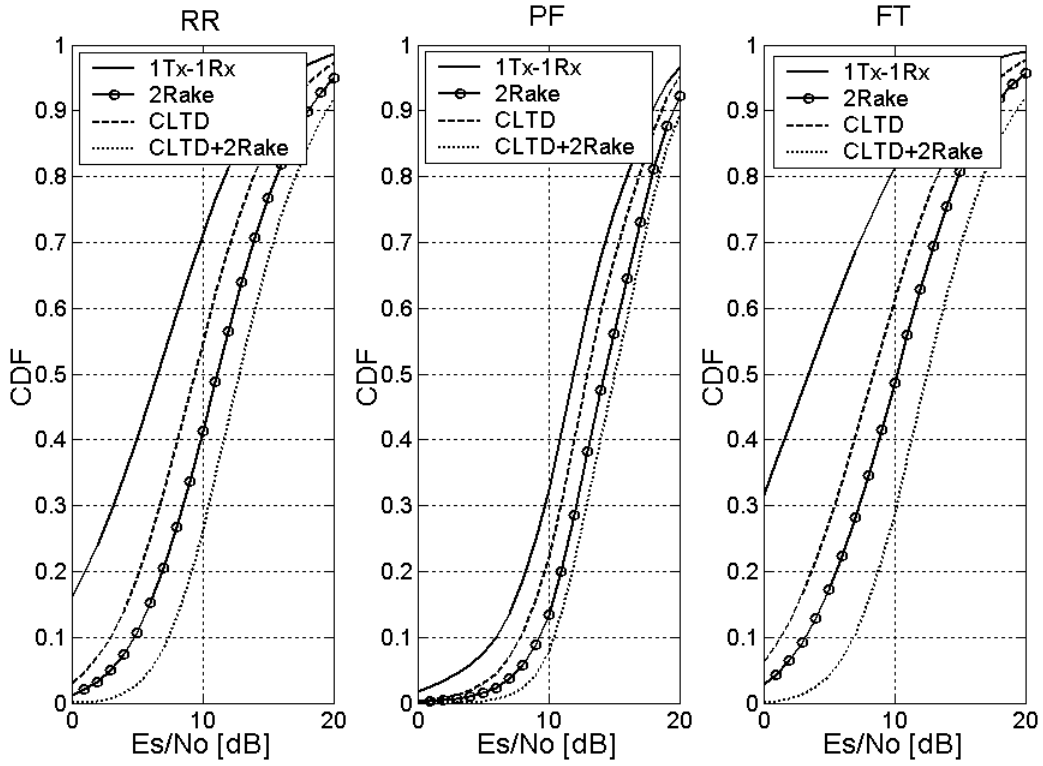

Figure 3.14 E_S/N_0 distribution at the HS-DSCH.

As can be seen from this picture, the E_S/N_0 improvement from CLTD+2Rake, denoted *E_S/N_0_gain(CLTD+2Rake)*, is smaller than the combination of the gain figures obtained for both individual features, denoted *[E_S/N_0_gain(CLTD)+ E_S/N_0_gain(2Rake)]*. These figures for the E_S/N_0 gains at the 50% quantile of the CDF are summarized in Table 3.5. As can be seen in the Table, the difference between *[E_S/N_0_gain(CLTD)+ E_S/N_0_gain(2Rake)]* and *E_S/N_0_gain(CLTD+2Rake)* is larger for FT. As explained in the previous Sections, this is due to the fact that this scheduler is the one for which the antenna schemes bring the largest diversity protection into the E_S/N_0 statistics. Thus, there is a significant proportion of the E_S/N_0 gain that is due to diversity protection. As a consequence, the larger difference between *E_S/N_0_gain(CLTD+2Rake)* and *[E_S/N_0_gain(CLTD)+ E_S/N_0_gain(2Rake)]* is due to the overlapping of the two sources of diversity protection.

On the other hand, PF is the one for which this difference is smaller. The reason is that, in this case, the multi-user diversity introduced by the scheduler prevents the antenna schemes from adding a significant extra diversity protection. As a consequence, the improvement experienced by the E_S/N_0 values comes almost completely from the average E_S/N_0 gains. Since these average gains exploit different mechanisms, they do not overlap and it is possible just to add them. As a consequence, *E_S/N_0_gain(CLTD+2Rake)* is very near *[E_S/N_0_gain(CLTD)+ E_S/N_0_gain(2Rake)]*.

Table 3.5. Comparison of E_S/N_0 gains at the 50% quantile. Pedestrian A.

E_S/N_0 gain	RR	PF	FT
E_S/N_0_gain(CLTD)	2.9 dB	1 dB	4.9 dB
E_S/N_0_gain(2Rake)	4.7 dB	2.3 dB	6.8 dB
A = [E_S/N_0_gain(CLTD)+ E_S/N_0_gain(CLTD)]	7.6 dB	3.3 dB	11.7 dB
B = E_S/N_0_gain(CLTD+2Rake)	6.3 dB	3.1 dB	9.1 dB
A – B	**1.3 dB**	**0.2 dB**	**2.6 dB**

Table 3.6 shows a similar analysis for the HSDPA cell capacity gain. As can be seen, the achieved gain with 2Rake+CLTD is lower than the combination of the individual gains from 2Rake and CLTD. This is due to the already described behaviour of the effective E_S/N_0 at the shared channel, together with the non-linearity of the mapping of E_S/N_0 into throughput, which becomes more severe as the E_S/N_0 values increase. For the sake of simplicity, the HSDPA cell capacity gain figures are expressed as linear multiplicative factors. For example, a gain of 46% is expressed with a linear multiplicative factor of 1.46.

Like in the E_S/N_0 discussion, the scheduler with the largest difference between the throughput gain of CLTD+2Rake and the product of the two individual gains is FT, while the difference is rather small for PF.

Also for this case, in spite of the lower HSDPA cell capacity gain that PF experiences when CLTD+2Rake is selected, PF is still the scheduler with the largest absolute system throughput. Nevertheless, compared with the 1Tx-1Rx case, the gain of going from RR to PF drops from 90% to 17%, while the loss due to going from RR to FT drops from 31% to 7% when CLTD is implemented.

Table 3.6. Comparison of HSDPA cell capacity gains. Pedestrian A.

HSDPA cell capacity gain for:	RR	PF	FT
CLTD	1.46	1.12	1.83

2Rake	1.82	1.29	2.29
Product of the gains from CLTD and 2Rake	2.66	1.44	4.19
CLTD+2Rake	2.23	1.38	3.01

3.3.4 Throughput gain per UE

The throughput gain figures shown in the previous Sections give an indication of how the HSDPA cell capacity improves when transmit and/or receive diversity techniques are deployed. However, these numbers do not provide a full picture about what happens in the system, since the throughput gain does not affect all the regions in the cell in the same manner. In fact, the throughput gain is larger for those UEs at the cell edge, due to two already mentioned mechanisms:

- UEs at the cell edge (i.e., with a low G factor) obtain better diversity protection in their received E_S/N_0.
- UEs at the cell edge typically have lower individual throughput figures, which involve the use of lower MCS and allows for more spectral efficient mapping of E_S/N_0 gain into throughput gain.

Figure 3.15, Figure 3.16 and Figure 3.17 show the average UE throughput gain as a function of the G factor for all the packet scheduling strategies under study. The reported figures are for Pedestrian A and 3 kmph.

For example, CLTD+2Rake yields a HSDPA cell capacity gain of 123% for RR (see Table 3.4), while the average UE throughput gain for UEs with G=-4 dB is 320%.

As can be seen, for both RR and PF, the average UE throughput gain grows as the G factor diminishes. This is equivalent to a coverage gain, since UEs with low G-factor are primarily located far from the Node-B.

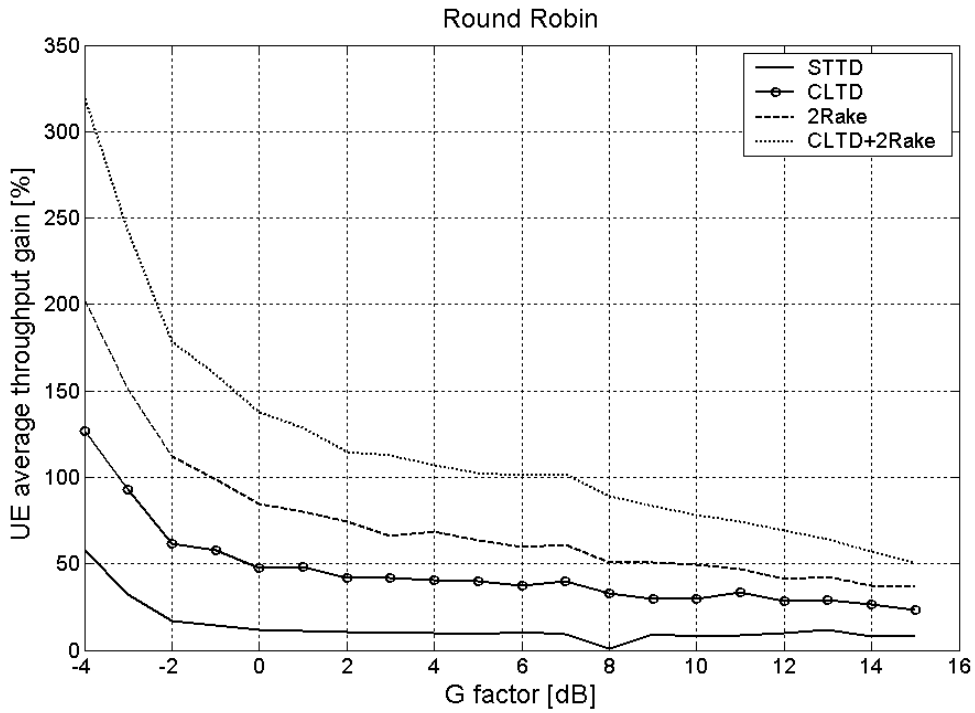

Figure 3.15 Average UE throughput vs. G factor for RR.

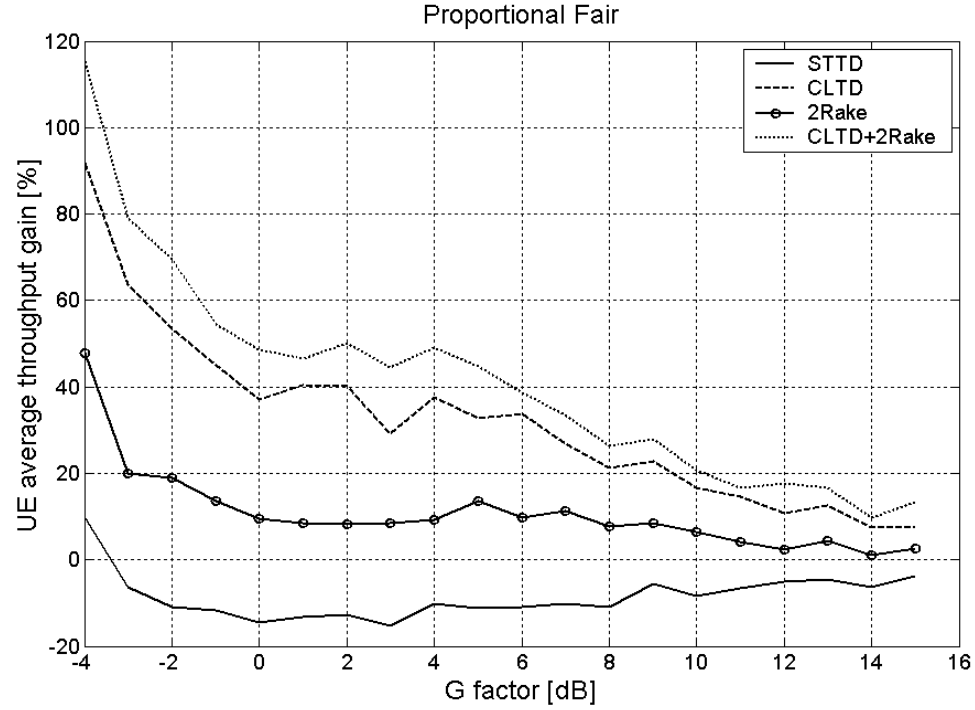

Figure 3.16 Average UE throughput vs. G factor for PF.

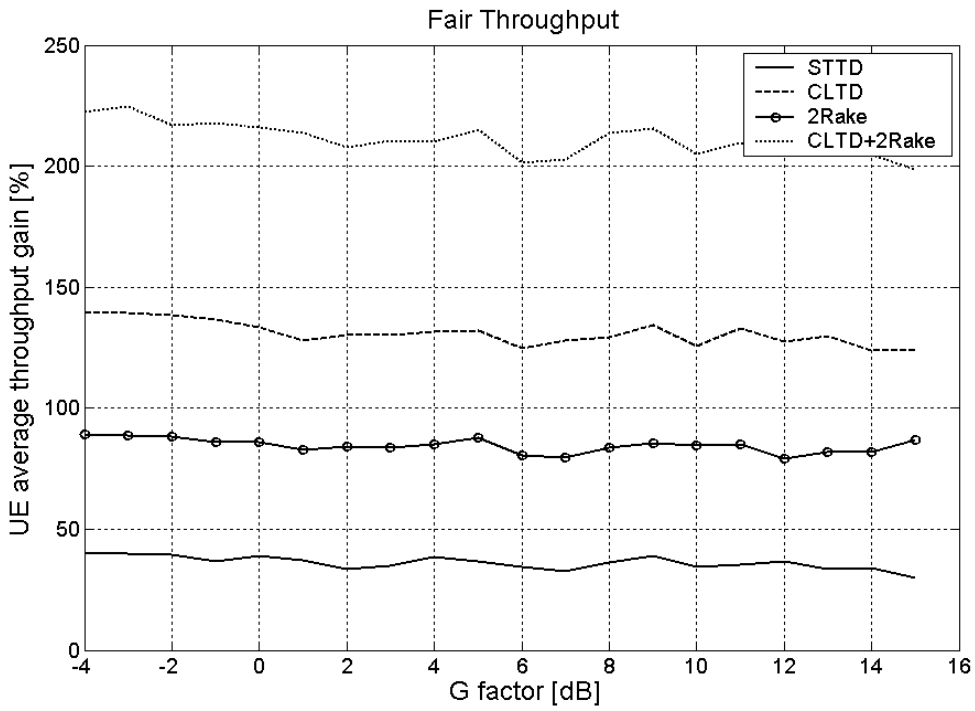

Figure 3.17 Average UE throughput vs. G factor for FT.

Moreover, it can be noticed that the average UE throughput gain is lower for PF, compared to RR. Again, this is due to two reasons:

- PF involves larger throughput figures, since the UEs are scheduled on the top of a constructive fade. As a consequence, higher order MCS are used and the system is less efficient when mapping E_S/N_0 gain into throughput gain.
- PF is not meant to take advantage from the E_S/N_0 diversity protection, since the involved stabilisation of the radio channel degrades the channel quality on the top of the constructive fades. As it can be seen, STTD yields a loss for almost all the values of the G factor.

Furthermore, the same UE throughput gain is observed for all the G factors in the case of FT, which is in coherency with the philosophy of this scheduler.

3.3.5 Impact of the maximum number of UEs in the queue

All the simulation results presented so far have been obtained for a queue size of 32 (see Table 3.3). This number is considered sufficiently high to provide enough multi-user diversity in the system. Under these circumstances, PF is always able to find a UE on the top of a constructive fade, and therefore it can yield the significant HSDPA cell capacity gain figures that have been reported.

In the following subsection, the dependence of the performance of PF upon the maximum number of UEs in the service queue is addressed; with special emphasis on how the deployment of transmit and receive diversity techniques affects this behaviour.

Figure 3.18 shows the HSDPA cell capacity for PF as a function of the maximum number of UEs in the queue. As can be seen, the HSDPA cell capacity increases as the maximum queue size grows, due to the larger multi-user diversity. However, this growth is not indefinite, since the system performance tends to saturate at some point. Throughout this Section, it has been claimed that, for the utilised settings (queue size equal to 32), STTD yields a loss when used with PF scheduling. In this plot, it can be seen that this statement is true from a queue size of five onwards, i.e., when the queue has room for very few UEs, the PF scheduler does not enjoy enough multi-user diversity. As a consequence, it cannot schedule UEs only on the top of constructive fades, but it has to serve UEs also in lower regions of their fading dynamic range. In such regions, STTD is not statistically worse than 1Tx1Rx and, thus, it can provide some gain.

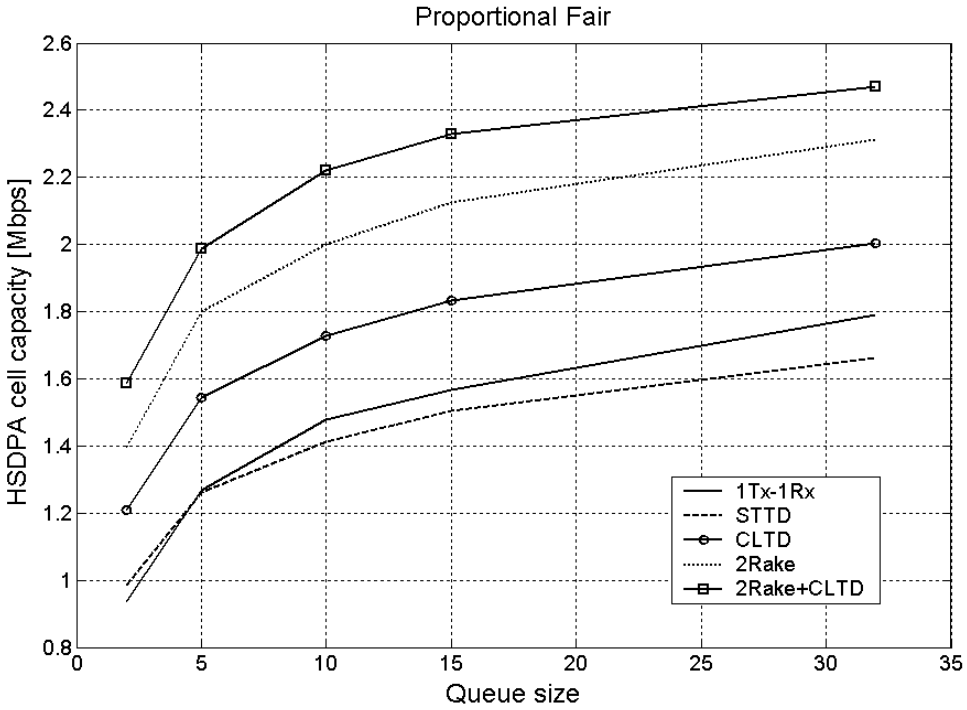

Figure 3.18 HSDPA cell capacity vs. maximum queue size for PF and Pedestrian A.

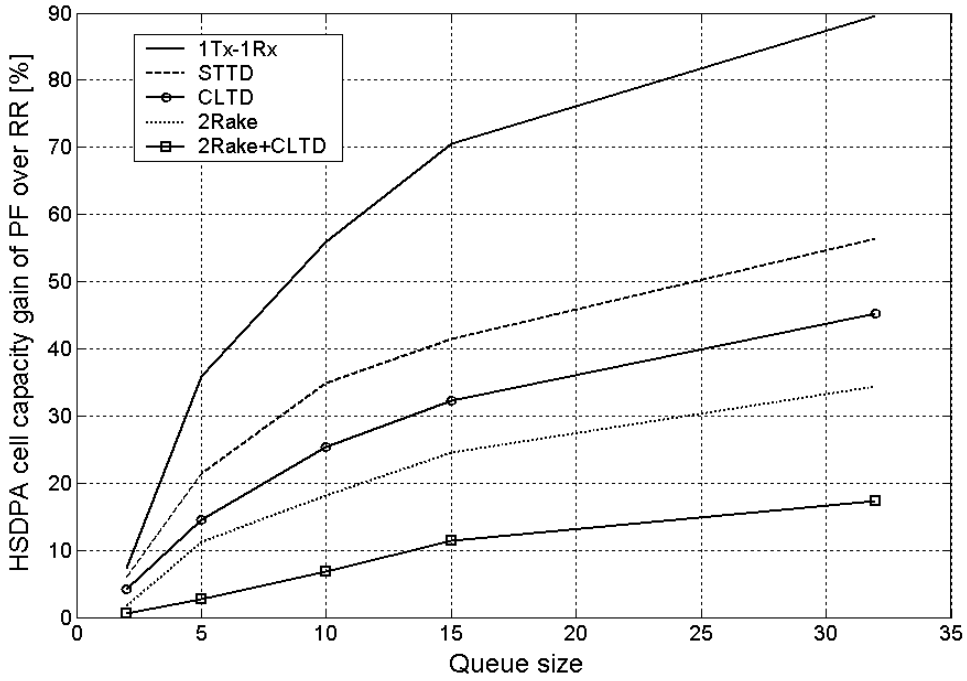

Figure 3.19 Gain of PF over RR vs. maximum queue size for Pedestrian A.

Figure 3.19 shows how the HSDPA cell capacity gain of PF over RR evolves with the maximum number of UEs in the queue. Notice that such gain diminishes when the maximum queue size decreases, due to the lower multi-user diversity. Moreover, as more advanced transmit and receive diversity schemes are deployed, the gain from having PF becomes lower. Such conclusion has already been pointed out in this study. Furthermore, the information in this curve adds the fact that the gain from multi-user diversity saturates for a lower number of UEs when more advanced antenna schemes (providing stronger channel stabilisation) are introduced.

3.3.6 Sensitivity analysis towards the UE speed

As already mentioned in this Section, the operations of PF scheduling and LA are based on CQI reports, for whose application there is a certain processing and transmission delay. These delays, together with the ones affecting the application of the transmission weights in CLTD, make the system performance sensitive to the UE speed. Figure 3.20 shows the evolution of the HSDPA cell capacity as a function of the UE speed for RR and Pedestrian A. As can be seen, the system performance degrades when the UE speed increases. Note that, since this curve is depicted for RR, the only delays affecting the system in this case are the ones for LA and the transmission weights of CLTD.

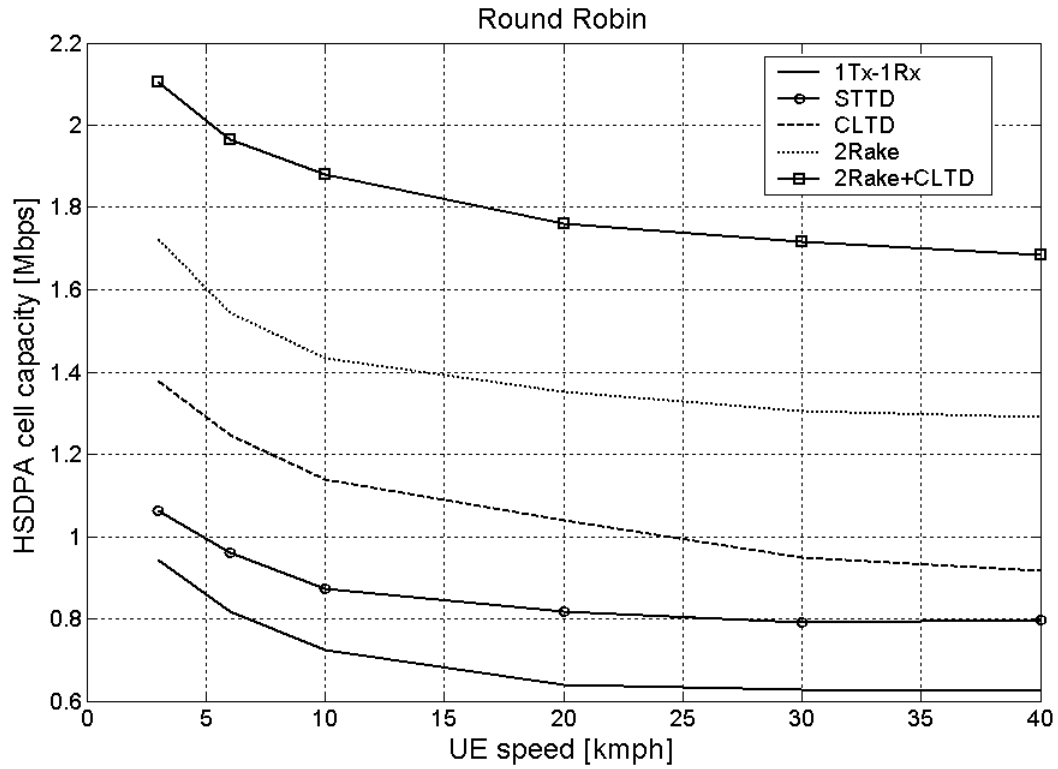

Figure 3.20 Gain of PF over RR vs. maximum queue size for Pedestrian A.

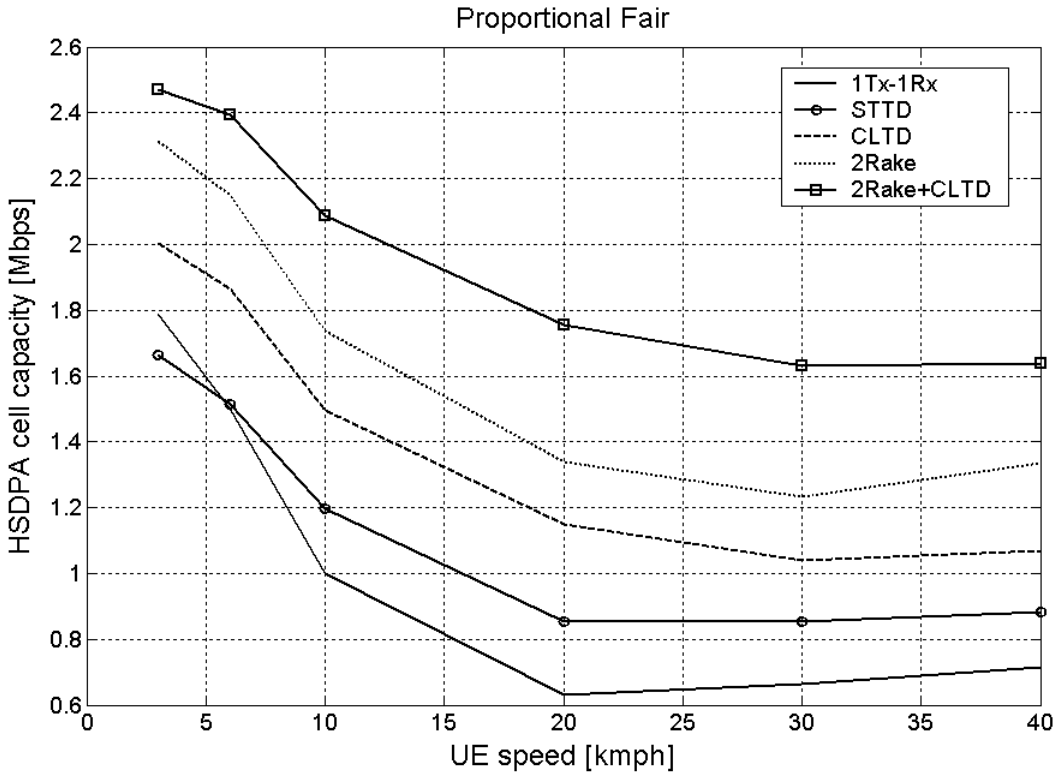

Figure 3.21 Gain of PF over RR vs. maximum queue size for Pedestrian A.

Figure 3.21 shows the same information for PF, which is also heavily affected by the delays in the packet scheduling process.

As can be seen in these figures, the degradation of the HSDPA cell capacity when the UE speed increases is larger for PF, since a CQI-delay dependent scheduling strategy is introduced. In addition, the difference between antenna schemes, in terms of how heavily they are affected by increasing the UE speed, is more exaggerated. For example, with RR, both 1Tx-1Rx and STTD experience a throughput reduction when the UE speed grows, but this reduction does not prevent STTD from always providing a gain over 1Tx-1Rx. However, for PF there is a change in the tendency when the UE speed grows: For low speeds, STTD yields a loss compared with 1Tx-1Rx. Nonetheless, for larger speeds, the stabilisation of the radio channel provided by STTD leads to a situation in which STTD offers a HSDPA cell capacity gain compared with 1Tx-1Rx. This is due to the fact that the lower power gradient of the radio channel makes the packet scheduling more robust towards the UE speed. Similar trends are observed in [20].

Table 3.7 summarises the relative degradation of the system throughput when going from 3 to 40 kmph. For both schedulers, the antenna scheme yielding the largest degradation for high UE speeds is 1Tx-1Rx, since it does not have any artificial stabilisation of the radio channel and, thus, suffers from larger variations in the experienced E_S/N_0 values. On the other hand, CLTD+2Rake is always the scheme with the lowest degradation, due to the fact that both the CLTD and the 2Rake features contribute to reduce the power gradient of the radio channel. As a consequence, there are smaller E_S/N_0 variations and the net impact of the delays under study is less harmful. Another trend that can be observed is that PF is more sensitive than RR towards the UE speed, since it obtains its gain from scheduling the UEs with the best instantaneous normalised channel quality. When the delays become relatively significant (i.e., at high UE speeds), the capability of the system to track the instantaneous channel quality of the different UEs is seriously jeopardised.

Table 3.7. System throughput degradation when going from 3 to 40 kmph. Pedestrian A.

Antenna scheme	Throughput reduction for RR	Throughput reduction for PF
1Tx-1Rx	34%	60%
STTD	25%	47%
CLTD	33%	47%
2Rake	25%	42%

CLTD+2Rake	20%	34%

Note that that the reported throughput degradation is dominated by the CQI signalling delay, since the feedback delay for CLTD is smaller. The latter is the main reason why the relative throughput loss for CLTD does not significantly exceed the loss for the other antenna configurations with an equivalent diversity order.

3.3.7 Performance under frequency selective channels

In this subsection, results for the case of Vehicular A at 3 kmph are presented in order to discuss the influence of frequency selective channels on the system performance. Table 3.8 shows the HSDPA cell capacity for all the considered antenna schemes and scheduling strategies under the aforementioned conditions. Note that the throughput figures are larger for Pedestrian A (compare Table 3.4 with Table 3.8), mainly due to the fact that this channel profile provides more orthogonality between signals transmitted from the same Node-B.

Table 3.8. Results for Vehicular A and 3 kmph.

Scheme	RR			PF			FT		
	HSDPA cell capacity [Mbps]	HSDPA cell capacity [Mbps]	HSDPA cell capacity [Mbps]	HSDPA cell capacity [Mbps]	HSDPA cell capacity [Mbps]	HSDPA cell capacity [Mbps]	HSDPA cell capacity [Mbps]	HSDPA cell capacity [Mbps]	HSDPA cell capacity [Mbps]
1Tx-1Rx	0.712	0%	0%	1.079	0%	52%	0.635	0%	-11%
STTD	0.695	-2%	0%	0.918	-15%	32%	0.652	3%	-6%
CLTD	0.891	25%	0%	1.176	9%	32%	0.857	35%	-4%
2Rake	1.206	69%	0%	1.457	35%	21%	1.158	83%	-4%
CLTD+2 Rake	1.403	97%	0%	1.552	44%	11%	1.359	114%	-3%

In RR, the Vehicular A case shows less HSDPA cell capacity gain when advanced transmit and receive diversity techniques are used. The reason is that the frequency diversity provided by the radio channel prevents the antenna diversity techniques from being able to bring so much gain into the system. Moreover, the average E_S/N_0 gain obtained in CLTD is lower, due

to the lack of degrees of freedom to fully adapt the transmission weights to the channel characteristics. However, even though the E_S/N_0 improvement is larger for Pedestrian A, this effect is partially compensated because this channel yields higher throughput, which involves a more frequent use of 16QAM and thus degrades the capability to map the E_S/N_0 gain into throughput gain. This effect is less exaggerated than in the case of PF, where the difference in throughput between the two channel profiles for 1Tx-1Rx is much larger. In fact, with PF and 1Tx-1Rx, the system throughput for Pedestrian A is 66% larger than that of Vehicular A, while this difference is down to 33% for RR. Apart from the orthogonality issues, which also affect the RR case, the significantly larger difference for PF is due to the fact that this algorithm schedules the UEs experiencing constructive fading, which is less beneficial when the dynamic range of the radio channel is reduced, for example due to the frequency selectivity of the Vehicular A channel profile. As a consequence, there is a noticeable difference in the linearity of the mapping between E_S/N_0 and throughput, which allows the Vehicular A map the E_S/N_0 changes into throughput changes in a more efficient manner.

For FT, the system also experiences less throughput gain (compared to the Pedestrian A case) when deploying advanced transmit and receive diversity techniques, due to the reasons already exposed for RR. Regarding the throughput degradation of FT compared with RR, it becomes lower in Vehicular A, due to the much larger frequency diversity protection experienced by the UEs at the cell edge, which makes it not so harmful to provide equal throughput in the entire cell. As already mentioned in this Section, UEs at the cell edge benefit from any extra source of diversity to a larger extent than those near the Node-B. Since FT focuses more resources on UEs at the cell edge than RR, the benefit (in terms of diversity) of having a frequency selective channel is stronger in FT, which lowers the difference between both schedulers in terms of HSDPA cell capacity.

Regarding the orthogonality degradation, this is also less important for UEs at the cell edge, since their received fraction of own cell interference (the only one subject to orthogonality effects) is lower. Again, this results in lower degradation for FT (compared with RR), since this schedulers focuses more resources on UEs at the cell edge.

When STTD is enabled together with PF in Vehicular A, there is smaller E_S/N_0 penalty, because the system was already having some frequency diversity. However, due to the larger linearity, this smaller degradation is mapped into a larger HSDPA cell capacity reduction (15%) than in Pedestrian A (7%).

When 2Rake is enabled with PF and Vehicular A, the average E_S/N_0 gain is the same as in Pedestrian A (3dB), and the E_S/N_0 penalty on the top of the constructive fades is lower. As a consequence, the effective E_S/N_0 gain from deploying 2Rake receivers with Vehicular A is larger. This phenomenon, together with the more linear mapping between E_S/N_0 and throughput, leads to a larger throughput gain for PF schedulers from deploying 2Rake receivers in a Vehicular A environment (35%, compared to the 29% gain achieved for Pedestrian A). The MCS selection probability for both channel profiles is depicted in Figure 3.22.

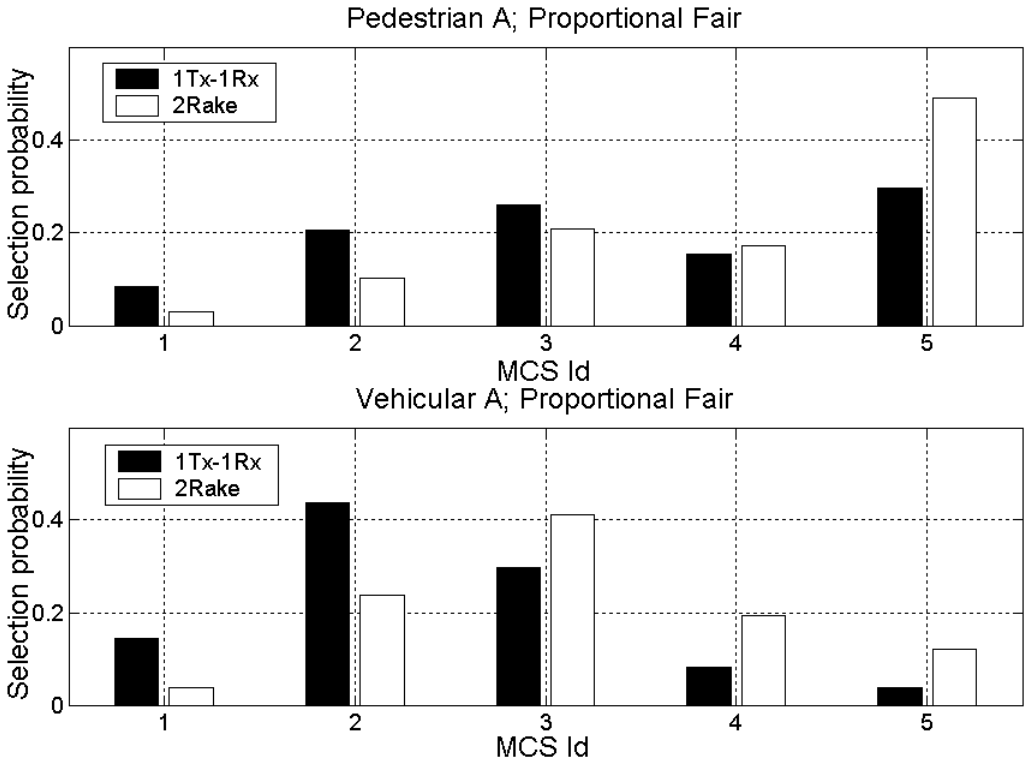

Figure 3.22 MCS selection probability of 1Tx-1Rx and 2Rake with PF scheduling for both Pedestrian A and Vehicular A.

A similar trend is observed when CLTD+2Rake is enabled, in spite of the fact that the obtained average E_S/N_0 gain is lower for Vehicular A, due to the aforementioned lack of degrees of freedom. However, this issue does not cause an inversion in the tendency, since the average E_S/N_0 gain is dominated by the contribution of the 2Rake receiver, due to the coarse quantisation of the channel weights in CLTD, which consist of four possible phase shifts without any amplitude modification.

For CLTD, most of the effects mentioned when discussing the case of 2Rake are still valid. However, due to the lack of degrees of freedom to adapt the transmission to the frequency selective channel, the average E_S/N_0 gain is lower. As a consequence, the gain from enabling CLTD with PF is slightly lower than in the Pedestrian A case (9%, compared to the 12% gain of Pedestrian A).

3.3.8 Simulation results for lower outage levels

In the previous Sections, the system performance has been analysed from a pole capacity perspective, i.e., the offered load is significantly larger than the system capacity. In this Section, extra simulation results are presented, in which the HSDPA cell capacity is presented as a function of the outage in the system. For these simulations, the selected environment is Pedestrian A at 3 kmph.

In this context, the outage in the system is defined as the proportion of UEs that are either blocked, dropped according to the criterion presented in Subsection 3.2.7, or admitted into the system but served with less than 64 kbps during their overall packet call.

Figure 3.23, Figure 3.24 and Figure 3.25 show the HSDPA cell capacity as a function of the outage for the different packet schedulers and antenna techniques.

For RR and PF, when the offered load is very high, UEs are served less often, which means that those UEs with poor radio conditions receive very low throughput, resulting in more outage if they are dropped or get less than 64 kbps. However, when the offered load is lower, there are typically less UEs in the queue and all of them have the chance to get access to more resources, which decreases the outage figures. In addition, when the offered load is too high, the service queue is likely to be full, which results in UEs getting blocked and the subsequent increase of the outage.

In the case of FT, the situation is special, since the scheduler is designed to deliver the same UE throughput in the entire cell. Therefore, if too many UEs are admitted in the system and it is not possible to deliver the minimum throughput to all of them, they are all counted for the outage statistics. This is due to the uniformity in the delivered quality of service, which makes the curve depicted in Figure 3.25 look almost like a step function. With FT, the scheduler is either capable to provide at least the minimum throughput (64 kbps) to all the UEs or unable to deliver this service to any of them. However, in Figure 3.25, the effects of both dropped and blocked calls are also included, which slightly smoothens the curves.

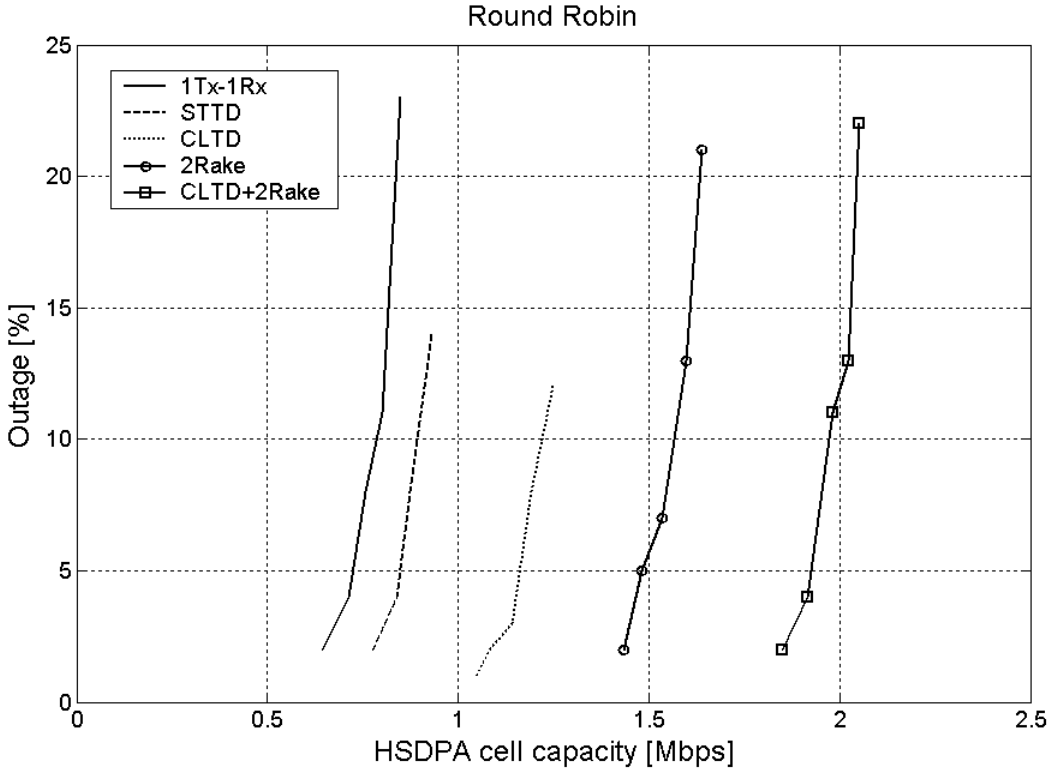

Figure 3.23 HSDPA cell capacity vs. outage for RR.

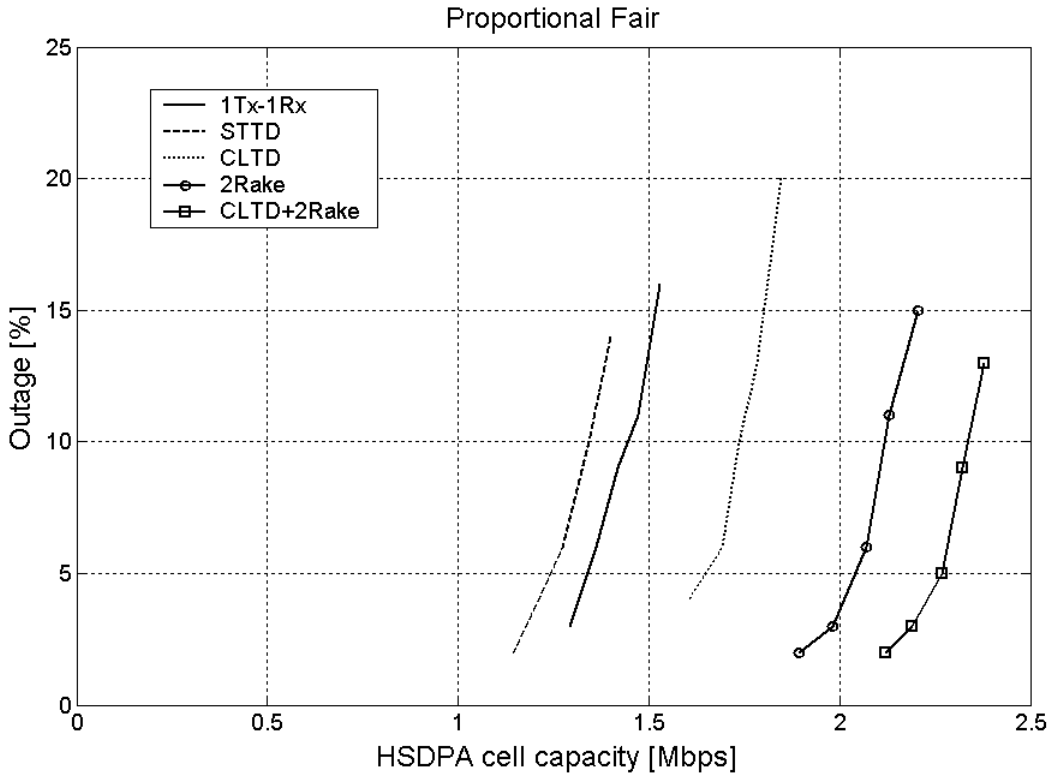

Figure 3.24 HSDPA cell capacity vs. outage for PF.

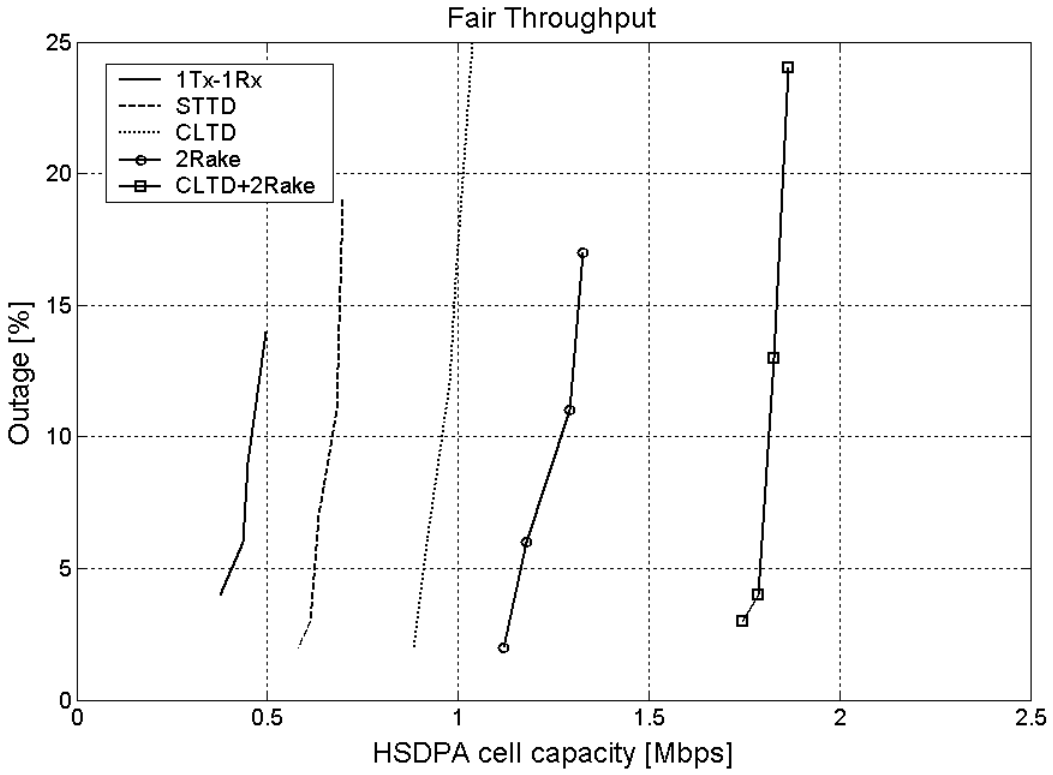

Figure 3.25 HSDPA cell capacity vs. outage for FT.

As can be seen, at e.g. 10% outage, the capacity gain from deploying CLTD+2Rake with RR, PF and FT is 150%, 62% and 296% respectively, while it is 123%, 38% and 201% when the pole capacity is considered. The reason for this is the fact that the lower outage is specially benefiting those UEs with low G factor, since these UEs tend to stay longer in the system. Due to the lower offered load, there are periods with less than 32 UEs in the queue, which forces the system to serve these low G factor UEs more often. As stated before in this Section, UEs with low G factor are able to extract the maximum benefit from the deployment of advanced antenna techniques, and this is the reason why the HSDPA capacity gain from deploying such techniques grows for lower outage levels.

3.4 Concluding remarks

In Task 1b.) the system performance of different transmit and receive diversity techniques has been analysed under different packet scheduling strategies within the framework of the HSDPA concept of UMTS. In general, it has been shown that there is strong interaction between the performance of these advanced antenna techniques and the selected packet scheduling strategies.

RR, FT and PF have been compared for all the antenna diversity schemes and the outcome is that the deployment of such advanced antenna concepts is more profitable (in terms of system throughput gain) in FT. This is mainly due to two reasons: (i) the FT scheduler allocates most of the resources to UEs at the cell edge, which are the ones benefiting more from the extra diversity in terms of E_S/N_0 stabilisation, and (ii), due to the focus on UEs with poor channel conditions, the subsequent lower system throughput leads to the use of lower MCS, which allows for more spectral efficient translation of E_S/N_0 gain into throughput gain.

On the other hand, the scheduler for whom the deployment of advanced antenna techniques yields the lowest performance gain is PF. Again, two main reasons have been identified for this behaviour: (i) the idiosyncrasies of the PF strategy makes it schedule UEs primarily when they are on the top or a constructive fade, which makes it not very advisable to stabilise the radio channel by increasing its diversity order; and (ii), PF yields much higher system throughput in the single antenna case, which leads to the utilization of higher order MCS, with the subsequent non-linearity and lack of efficiency when mapping E_S/N_0 gain into throughput gain.

A sensitivity analysis towards the UE speed has been conducted. It revealed that PF is much more sensitive than RR to the UE speed. The reason for this is that RR does not require any fast information of the instantaneous state of the radio channel in order to conduct the scheduling, while this is not the case for PF. Another important finding is that the deployment of transmit and receive diversity techniques makes the system more robust towards the UE speed, i.e., towards the negative impact of the delays. For example, at low speeds, STTD gives a loss compared with 1Tx-1Rx, due to the degradation of the channel conditions on top of the constructive fades for STTD. However, as the UE speed grows, the extra robustness against speed provided by STTD makes the fast scheduling process perform better to such an extent that STTD starts giving a gain over 1Tx-1Rx.

Both the interaction between the deployment of STTD with fast scheduling and the impact of the UE speed on the system performance in this case have been addressed in a simplified theoretical study, which shows the same trends as the simulation results.

Furthermore, extra simulation results are presented and analysed in order to illustrate the influence of the maximum number of UEs on the achievable multi-user diversity. These results clearly show how the benefit from fast scheduling grows with the number of UEs eligible for selection. In addition, it is also shown how the gain from multi-user diversity saturates beyond a certain number of UEs.

In order to show how the presented performance figures evolve when the system is operated under frequency selective channels, some simulation results in frequency selective environments have been obtained and discussed. Though in general both the average and diversity E_S/N_0 improvements due to the deployment of advanced antenna schemes are better for Pedestrian A, this does not necessarily mean that the same conclusion is valid for the HSDPA cell capacity gain. The reason for this difference in the tendency is that the E_S/N_0 improvements are more efficiently exploited in Vehicular A, due to the fact that the lower orthogonality forces a less frequent use of 16QAM.

The aforementioned analysis has been conducted for an offered load that is significantly above the system capacity. In the end, the system capacity has been shown as a function of the outage for all the considered scheduling strategies and antenna schemes. The outcome is that, although the main trends remain the same, the HSDPA cell capacity gain is larger when the system is operated at lower outage numbers, due to the fact that lower outage specially benefits those UEs with lower G factor, which are the ones exploiting the E_S/N_0 improvements in a more spectral efficient manner.

4 REFERENCES

[1] W. C. Jakes, "Microwave Mobile Communications", *IEEE Press*, 1974

[2] S. Parkvall, M. Karlsson, M. Samuelsson, L. Hedlund and B. Goransson, "Transmit diversity in WCDMA: link and system level results", *IEEE Proc. 51st Vehicular Technilogy Conference*, Vol. 2, pp. 864-868, May 2000.

[3] H. Holma, A. Toskala (Editors). "WCDMA for UMTS. Radio access for third generation mobile communications", Second edition, John Wiley & Sons, Ltd, England, August 2002.

[4] S.M. Alamouti. "A simple transmit diversity technique for wireless communications". *IEEE Journal on Selected Areas on Communications*, Vol. 16, No. 8, October 1998.

[5] G.J. Foschini. "Layered space-time architecture for wireless communication in a fading environment when using multi-element antennas". *Bell Labs Technical Journal*, Autumn, 1996.

[6] J. Ramiro-Moreno, K. I. Pedersen and P.E. Mogensen, "Radio resource management for WCDMA networks supporting dual antenna terminals", *IEEE Proc. 55th Vehicular Technology Conference*, Vol. 2, pp. 694-698, May 2002.

[7] A. G. Kogiantis, N. Joshi, O. Sunay, "On transmit diversity and scheduling in wireless packet data", *IEEE Proc. International Conference on Communications*, Vol. 8, pp. 2433 –2437, 2001.

[8] J.M. Holtzman, "Asymptotic Analysis of Proportional Fair Algorithm", *IEEE Proc. PIMRC*, pp. F33-F37, September 2000.

[9] F. Kelly, "Charging and Rate Control for Elastic Traffic", *European Transactions on Telecommunications*, Vol. 8, pp. 33-37, 1997.

[10] A. Jalali, R. Padovani, R. Pankaj, "Data Throughput of CDMA-HDR a High Efficiency-High Data Rate Personal Communication Wireless System", *IEEE Proc. 51st Vehicular Technology Conference*, pp. 1854-1858, May 2000.

[11] T.E. Kolding, F. Frederiksen, P. E. Mogensen, "Performance aspects of WCDMA systems with High Speed Downlink Packet Access (HSDPA)", *IEEE Proc. 56th Vehicular Technology Conference*, pp. 477-481, September 2002.

[12] S. Hämäläinen, P. Slanina, M. Hartman, A. Lappeteläinen, H. Holma, O. Salonaho, "A novel interface between link and system level simulations", *Proceedings of ACTS Summit 1997*, pp. 509-604, Aalborg, October 1997.

[13] H. L. Bertoni, "Radio propagation for modern wireless systems", *Prentice Hall PTR*, 2000.

[14] European Telecommunications Standards Institute, "Selection procedures for the choice of radio transmission technonogies for the UMTS", TR 101 112 (UMTS 30.03), Version 3.2.0, April 1998.

[15] F. Frederiksen, T.E. Kolding, "Performance and modeling of WCDMA /HSDPA transmission/H-ARQ schemes", *IEEE Proc. 56th Vehicular Technology Conference*, Vol. 1, pp. 472-476, May 2002.

[16] 3rd Generation Partnership Project, "Physical layer procedure", TS. 25.214, Version 5.3.0, Available online at www.3gpp.org, December 2002.

[17] S. Hämäläinen, H. Holma, K. Sipilä, "Advanced WCDMA radio network

simulator", *IEEE Proc. of the IEEE Symposium on Personal, Indoor and Mobile Radio Communications*, Osaka, September 1999.

[18] K. Miyoshi, T. Uehara, M. Kasapidis, K. Hiramatsu, M. Uesugi, O. Kato, "Link adaptation method for HSDPA for W-CDMA", *Proceedings of WPMC-01*, Aalborg, Denmark, September 2001.

[19] R. C. Elliot, W.A. Krzymien, "Scheduling algorithms for the cdma2000 packet data evolution", *IEEE Proc. 56th Vehicular Technology Conference*, Vol. 1, pp. 304-310, September 2000.

[20] L. T. Berger, L. Schumacher, J. Ramiro-Moreno, P. Ameigeiras, T. E. Kolding, P. E. Mogensen, "Interaction of transmit diversity and proportional fair scheduling", *IEEE Proc. 57th Vehicular Technology Conference*, May 2003.

[21] Mika Ventola, Esa Tuomaala, Pekka A. Ranta, "Performance of dual antenna diversity reception in WCDMA terminals", *IEEE Proc. 57th Vehicular Technology Conference*, May 2003.

[22] Medbo J., Hallenberg H. and Berg J.-E., "Propagation characteristics at 5 GHz in typical radio-LAN scenarios", *Proceedings of IEEE 49th Vehicular Technology Conference*, vol. 1, July 1999, pp. 185–189.